DOI: 10.1002/ejoc.200901070

Synthesis of Triazole-Bridged Unsymmetrical Porphyrin Dyads and Porphyrin–Ferrocene Conjugates

Vijayendra S. Shetti[a] and Mangalampalli Ravikanth*[a]

Keywords: Click chemistry / Energy transfer / Electron transfer / Azides / Sandwich complexes / Porphyrinoids

A simple method has been used to synthesize four porphyrin azides with cores such as N_4, N_3S, N_2SO and N_2S_2 in 60–90 % yields by treating the corresponding aminoporphyrins with *tert*-butyl nitrite (*t*BuONO) and azidotrimethylsilane ($TMSN_3$) in THF/CH_3CN under mild reaction conditions. The hitherto unknown aminoporphyrins with heteroatom cores were synthesized from their corresponding nitroporphyrins by standard $SnCl_2$/HCl reduction. The azidoporphyrins were used to synthesize six triazole-bridged unsymmetrical porphyrin dyads containing two different types of porphyrin sub-units as well as five triazole-bridged porphyrin–ferrocene conjugates under Cu^I-catalyzed "click" reaction conditions. Various Cu^I-catalyzed reaction conditions were studied and the best yields of triazole-bridged dyads and conjugates were obtained with CuI/DIPEA in THF/CH_3CN at room temperature for overnight. The unsymmetrical porphyrin dyads and porphyrin–ferrocene conjugates were characterized by various spectroscopic and electrochemical techniques. In unsymmetrical porphyrin dyads, the NMR, absorption and electrochemical studies indicate a weak interaction between the two porphyrin sub-units. However, preliminary photophysical studies support an efficient singlet-singlet energy transfer from one porphyrin unit to another in five unsymmetrical dyads reported here. In porphyrin–ferrocene conjugates, the fluorescence of porphyrin was quenched significantly due to photo-induced electron transfer from ferrocene to porphyrin.

Introduction

Sharpless and co-workers[1] discovery of copper(I)-catalyzed variant of Huisgen's 1,3-diploar cycloaddition of azides and alkynes to afford 1,4-disubstituted 1,2,3-triazoles under mild conditions, popularly known as "click chemistry" has resulted in explosive growth of research articles and reviews[2] describing the wealth of applications of this practical and sensible approach in various research fields including bioconjugation, materials science and drug discovery. The advantages of Cu^I-catalyzed "1,3-dipolar" cycloaddition reactions are: (1) to afford the 1,4-regioisomer exclusively with minimum work-up and purification, (2) to increase the reaction rate, (3) to eliminate the need for elevated temperatures and (4) favourable reaction conditions for variety of functional groups. Although the Cu^I-catalyzed cycloaddition reaction is versatile and extensively used, reports on the applications of this methodology to porphyrin chemistry is still in their infancy. There are some reports on triazole-appended porphyrin systems[3] but reports on triazole-bridged porphyrin dyads[4] and other conjugates synthesized under Cu^I-catalyzed cycloaddition reactions are very scarce (Figure 1). Chen and co-workers[4a] reported the synthesis of a β-*meso*-1,2,3-triazole-linked Ni^{II} derivative of the bis-porphyrin (**I**) by coupling the Ni^{II} derivative of β-azidotetrarylporphyrin with the Ni^{II} derivative of *meso*-ethynyldiphenylporphyrin in DMF in the presence of $CuSO_4 \cdot 5H_2O$/ascorbic acid at 50 °C. Odobel and co-workers[4b] explored various Cu^I-catalyzed conditions to synthesize triazole-bridged metalloporphyrin dyads (**II**) and found that copper carbene [*N*,*N*′-bis(2,4,6-trimethylphenyl)-4,5-dihydroimadazol-2-ylidene]CuBr in the solvent mixture THF/water (3:1) was the better catalyst to afford triazole-bridged dyads. We recently reported[4c] on the first synthesis of a triazole-bridged unsymmetrical porphyrin dyad (**III**) under click reaction conditions by reacting 21,23-dithiaporphyrin (N_2S_2 core) containing an alkyne functional group and a normal porphyrin (N_4 core) containing an azide functional group in the presence of sodium ascorbate and $CuSO_4$ in a water/acetone mixture at 80 °C for four days. Except for the above-mentioned communications, to the best of our knowledge there are no reports available on triazole-bridged porphyrin dyads. We have been involved in the synthesis of unsymmetrical dyads[5] containing two different porphyrin sub-units such as porphyrin and heteroporphyrin connected by various linkers with an aim to identify the best unsymmetrical porphyrin dyads showing maximum singlet–singlet energy transfer for various molecular electronic applications. During our studies, we realized that the bridging group connecting two different porphyrins plays an important role in energy transfer at singlet state. For example, the diphenylethyne-bridged porphyrin dyad containing N_4 and N_2S_2 porphyrin sub-units exhibited inef-

[a] Department of Chemistry, Indian Institute of Technology, Bombay, Powai, Mumbai 400076, India
E-mail: ravikanth@chem.iitb.ac.in

Supporting information for this article is available on the WWW under http://dx.doi.org/10.1002/ejoc.200901070.

ficient energy transfer from the N_4 porphyrin sub-unit to the N_2S_2 porphyrin sub-unit.[4c] However, in triazole-bridged porphyrin dyads containing N_4 and N_2S_2 porphyrin sub-units **III**, an efficient energy transfer from the N_4 porphyrin sub-unit to the N_2S_2 porphyrin sub-unit was observed.[4c] This result inspired us to synthesize more examples of triazole-bridged unsymmetrical porphyrin dyads containing two different porphyrin sub-units. In this paper, we present our detailed account on the synthesis of the diphenyl-1,2,3-triazole-bridged unsymmetrical porphyrin dyads **1**–**6** containing two different porphyrin sub-units such as N_4/ZnN_4–N_3S, N_4/ZnN_4–N_2S_2, ZnN_4–N_2SO, N_3S–N_2S_2 units (Figure 2) as well as 1,2,3-triazole-bridged porphyrin–ferrocene conjugates **7**–**11** (Figure 3) with N_4, N_3S, N_2S_2 and N_2SO cores under click reaction conditions. To synthesize the dyads and conjugates, we required the unknown *meso*-(azidophenyl)porphyrin building blocks with heteroatom-substituted porphyrin cores, which were synthesized from the corresponding aminoporphyrins by applying Moses reaction conditions[6] reported recently, and the aminoporphyrins were, in turn, synthesized from nitroporphyrins under standard $SnCl_2$/HCl conditions.[7] The NMR, absorption and electrochemical studies carried out on unsymmetrical porphyrin dyads **1**–**6** and porphyrin–ferrocene conjugates **7**–**11** support a weak interaction between the sub-units. The fluorescence studies indicate low fluorescence yields for porphyrin–ferrocene conjugates **7**–**11** because of photo-induced electron transfer from ferrocene to porphyrin and efficient singlet–singlet energy transfer from the porphyrin sub-unit to another in most of the triazole-bridged porphyrin dyads **1**–**6** reported here.

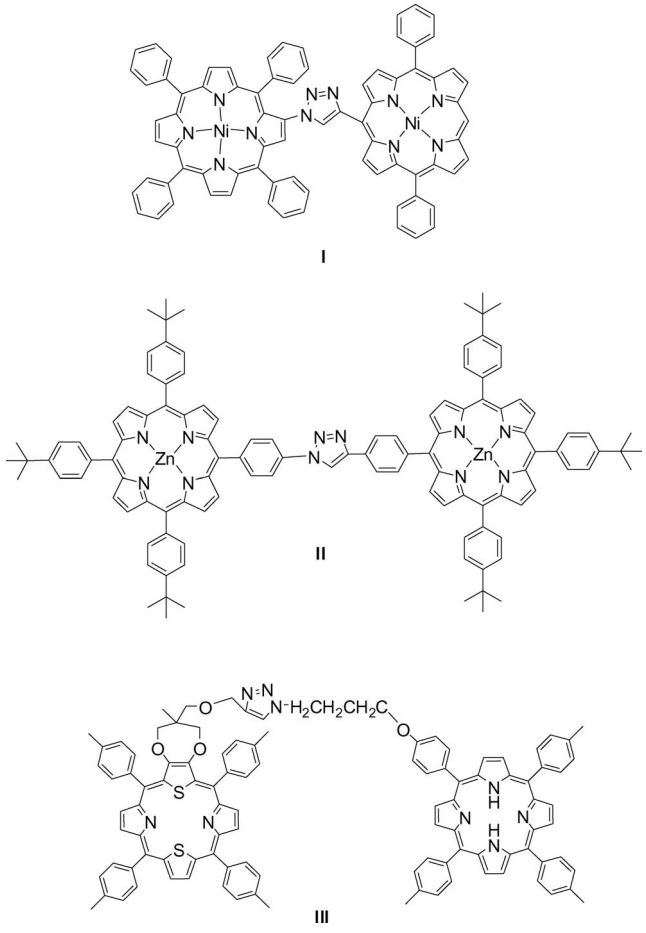

Figure 1. Triazole-bridged porphyrin dyads described in the literature.

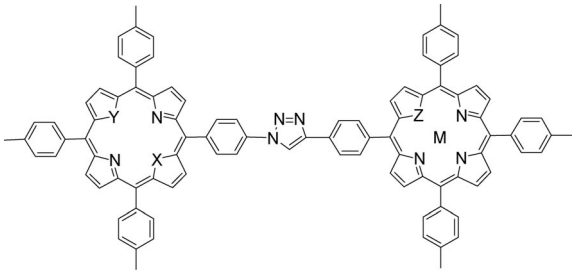

Figure 2. Various triazole-bridged unsymmetrical dyads synthesized in the present work.

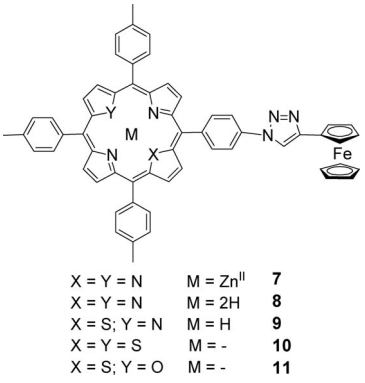

Figure 3. Various triazole-bridged porphyrin–ferrocene conjugates synthesized in the present work.

Results and Discussion

Mono *meso*-(*p*-Nitrophenyl)porphyrin Building Blocks with N_4 (12), N_3S (15), N_2S_2 (17) and N_2SO (19) Cores

The mono *meso*-(nitrophenyl)porphyrin building blocks with different cores **12**, **15**, **17** and **19** were prepared by following various approaches as outlined below. The mono *meso*-(*p*-nitrophenyl)porphyrin with N_4 core **12** was synthesized by mixed condensation[8] of one equivalent of *p*-nitrobenzaldehyde with three equivalents of *p*-tolualdehyde and four equivalents of pyrrole under Lindsey's porphyrin forming conditions[9] and afforded compound **12** in 10% yield (Scheme 1). The mono-*meso*-(*p*-nitrophenyl)porphyrins with N_3S (**15**), N_2S_2 (**17**) and N_2SO (**19**) cores were synthesized as presented in Scheme 1. The unsymmetrical thiophenediol[10] **14** was prepared in 48% yield by treating

2-(*p*-tolylhydroxymethyl)thiophene (**13**) with two equivalents of *n*BuLi followed by 1.2 equiv. of 4-nitrobenzaldehyde in THF at 0 °C. The 21-thiaporphyrin containing a *p*-nitrophenyl group in the *meso*-position **15** was prepared in 8% yield by condensing one equivalent of diol **14** with two equivalents of *p*-tolualdehyde and three equivalents of pyrrole under mild acid-catalyzed porphyrin-forming conditions.[9] The 21,23-dithiaporphyrin containing a *p*-nitrophenyl group in *meso*-position **17** was synthesized in 10% yield by condensing one equivalent of diol **14** with one equivalent of 16-thiatripyrrin[11] **16** in CH_2Cl_2 under mild acid-catalyzed conditions. The porphyrin **19** with N_2SO core containing *meso*-nitrophenyl group was synthesized similarly in 8% yield by condensing one equivalent of **14** with one equivalent of 16-oxatripyrrin[11] **18** under the same mild porphyrin-forming conditions. The porphyrins **12**, **15**, **17** and **19** were characterized by mass, NMR, absorption and fluorescence spectroscopic techniques. The molecular ion peak in mass spectra confirmed the identities of all four porphyrins. The ^{1}H NMR spectra showed characteristic signals expected for porphyrins **12**, **15**, **17** and **19**. The larger number of signals observed for pyrrole and thiophene protons for porphyrins **12**, **15**, **17** and **19** indicate the unsymmetric nature of these porphyrins. The absorption spectra of porphyrins **12**, **15**, **17** and **19** showed four Q-bands and one Soret band and peak positions were matching closely with their corresponding *meso*-tetratolylporphyrin analogues.[12]

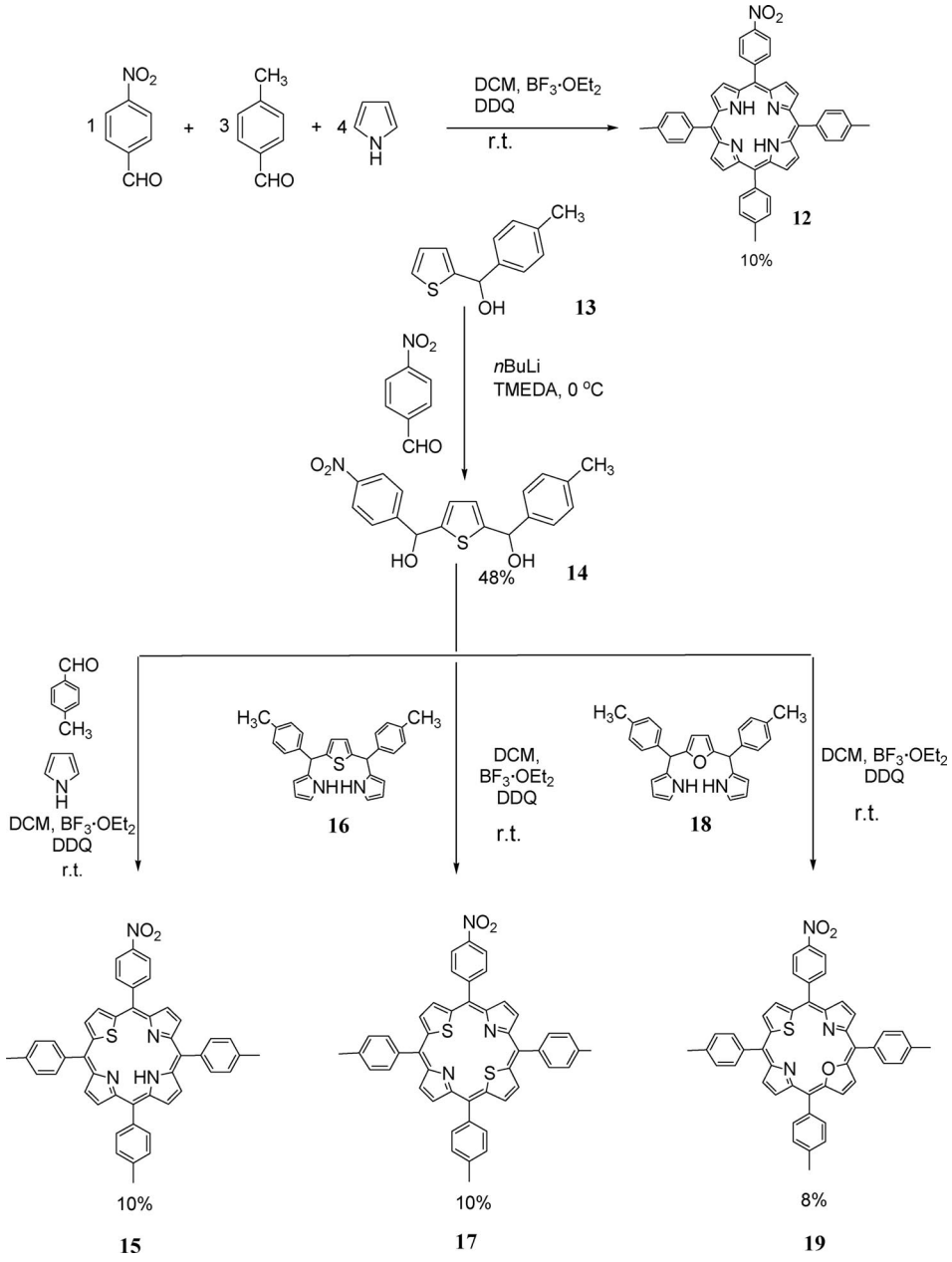

Scheme 1. Synthesis of *meso*-(*p*-nitrophenyl)porphyrins with N_4, N_3S, N_2S_2, N_2SO cores.

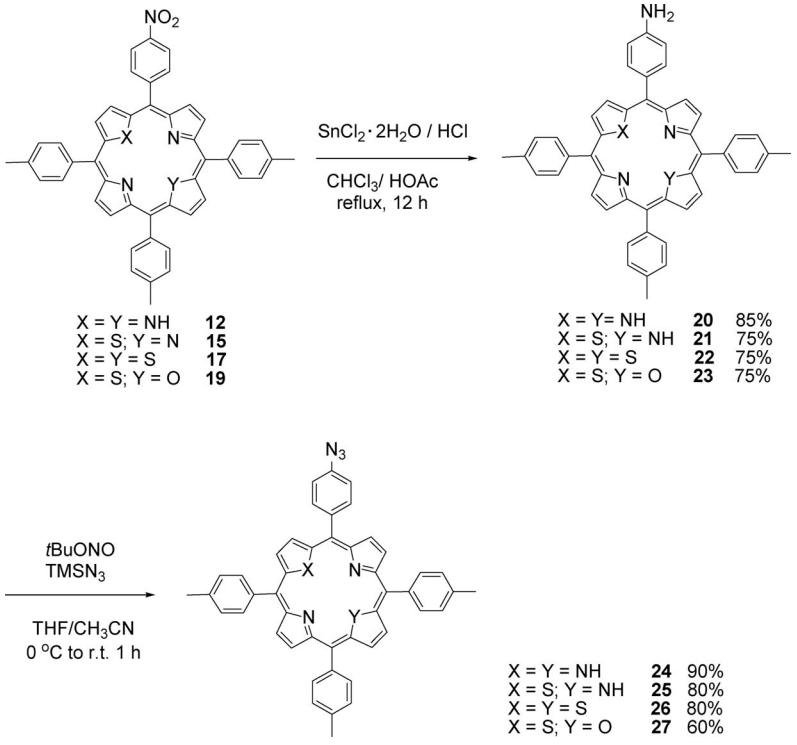

Scheme 2. Synthesis of *meso*-(*p*-aminophenyl)- and *meso*-(*p*-azidophenyl)porphyrins with N_4, N_3S, N_2S_2, N_2SO cores.

Mono *meso*-(*p*-Aminophenyl)porphyrin Building Blocks with N_4 20, N_3S 21, N_2S_2 22 and N_2SO 23 Cores

The mono *meso*-(*p*-aminophenyl)porphyrins with various porphyrin cores **20**–**23** were synthesized by reducing the nitro group of corresponding mono-*meso*(*p*-nitrophenyl)porphyrins **12**, **15**, **17** and **19**, respectively, with $SnCl_2$ in the presence of concd. aqueous HCl[7] (Scheme 2). Column chromatographic purification on silica afforded *meso*-(*p*-aminophenyl)porphyrins **20**–**23** in 75–85% yields. The *meso*-(aminophenyl)porphyrins **20**–**23** were confirmed by molecular ion peak in mass spectra and elemental analysis which was matching with the exact composition of amino porphyrins. In ^{1}H NMR spectra of aminoporphyrins **20**–**23**, a broad signal around 4.0 ppm indicated the presence of amino group. The absorption spectra of aminoporphyrins **20**–**23** showed four Q-bands and one strong Soret band with peak maxima were almost matching with those of nitroporphyrins.

Mono *meso*-(*p*-Azidophenyl)porphyrin Building Blocks with N_4 (24), N_3S (25), N_2S_2 (26) and N_2SO (27) Cores

The *meso*-(azidophenyl)porphyrins were prepared earlier by Odobel and others[4a,4b] from the corresponding amines via their diazonium salts. Although this method works efficiently, NaN_3 is toxic and explosive and needs to be handled carefully. Moses and co-workers[6] recently reported the synthesis of aromatic azides from their corresponding amines using stable, less hazardous and non-explosive reagents such as *tert*-butyl nitrite (*t*BuONO) and azidotrimethylsilane ($TMSN_3$) under mild reaction conditions. We employed Moses conditions to prepare *meso*-(azidophenyl)-porphyrins **24**–**27** in 60–90% yields by reacting *meso*-(aminophenyl)porphyrin with 1.5 equiv. of *t*BuONO followed by 1.2 equiv. of $TMSN_3$ in CH_3CN/THF (Scheme 2). Although the yields are in the same range as those obtained with standard NaN_3 method, we found that the reaction is simple, easy to handle and equally efficient to prepare azidoporphyrins in decent yields. The *meso*-(azidophenyl)-porphyrins **24**–**27** were confirmed by ES-MS mass which showed either M^+ or $(M - N_2)^+$ peak. In ^{1}H NMR, the absence of signal at δ = 4.00 ppm corresponding to the amino group confirmed the transformation of the amino group to an azido group. The absorption spectra of *meso*-(azidophenyl)porphyrins **24**–**27** showed four Q-bands and one Soret band and peak positions are almost matching with those of *meso*-(nitrophenyl)- and *meso*-(aminophenyl)-porphyrins.

Triazole-Bridged Unsymmetrical Porphyrin Dyads 1–6

To synthesize triazole-bridged click porphyrin dyads, we need an access to *meso*-(ethynylphenyl)porphyrin building blocks along with *meso*-(azidophenyl)porphyrin building blocks. The mono *meso*-(4-ethynylphenyl)porphyrin building blocks such as **28** (N_4 core), **29** (ZnN_4) and **30** (N_3S core) were synthesized by following the reported procedures.[5b,13] Using *meso*-(azidophenyl)porphyrin and *meso*-(ethynylphenyl)porphyrin building blocks, we carried out a series of 1,3-dipolar cycloaddition reactions under various reaction conditions to synthesize triazole-bridged

porphyrin dyads **1**–**6**. Initially, we attempted to synthesize the free-base porphyrin dyad **4** by click reaction conditions used by us earlier[4c] for preparation of N_4–N_2S_2 porphyrin dyad **III** (Figure 1) by reacting **24** and **28** in the presence of sodium ascorbate and $CuSO_4$ in a water/acetone mixture at 80 °C for four days. However, we noticed that the N_4 porphyrin **28** was metallated by copper under these reaction conditions which was not observed while preparing porphyrin dyad **III**. Odobel and co-workers[4b] also observed copper insertion problem during their investigations for the preparation of dyad **II**. Hence, to optimize the conditions, we carried out series of trial reactions using Zn^{II}-metallated N_4 ethynylporphyrin **29** with N_3S azidoporphyrin **25** under various reaction conditions. The porphyrins **25** and **29** were reacted under same click reaction conditions used for dyad **III** but the expected dyad **1** did not form. Further we modified the reaction conditions and reacted **25** and **29** in toluene in the presence of Diisopropylethylamine (DIPEA) and $CuSO_4{\cdot}5H_2O$/sodium ascorbate at room temperature for 7 d. We noticed the formation of dyad **1** in very trace amount after three days but no improvement in dyad **1** formation even after seven days. The first success in the synthesis of dyad **1** came when we used Odobel's reaction conditions[4b] by reacting **25** and **29** in THF/H_2O (1:5) in the presence of $Cu[P(OEt)_3]I$ at 50 °C for 12 h. The reaction worked smoothly and afforded dyad **1** in 45% yield. Since the catalyst $Cu[P(OEt)_3]I$[14] is not readily available, we then modified the conditions further by reacting **25** and **29** in THF/CH_3CN (1:1) in the presence of CuI/DIPEA at room temperature for 12 h. After simple work-up and flash column chromatographic purification on basic alumina, the dyad

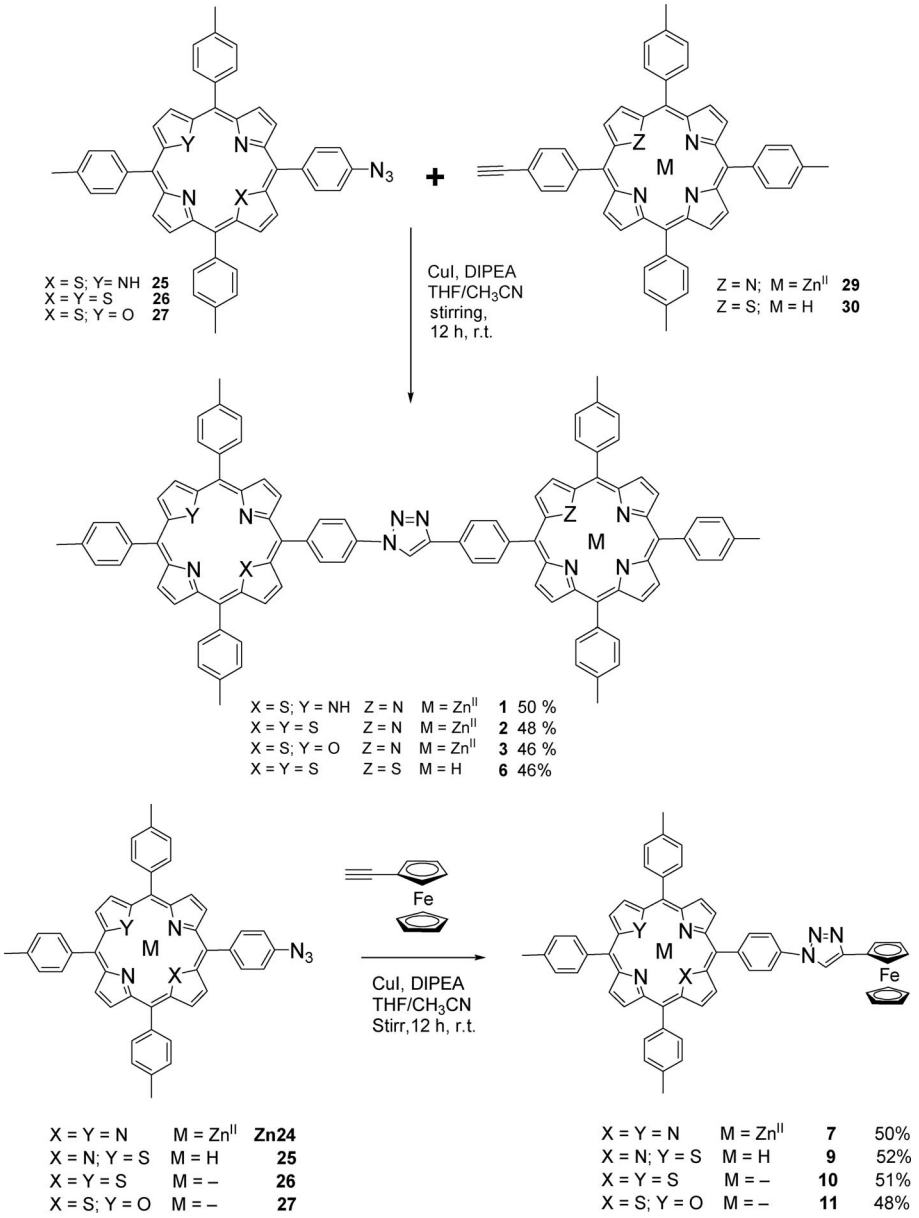

Scheme 3. Synthesis of triazole-bridged unsymmetrical porphyrin dyads and porphyrin–ferrocene conjugates.

1 was obtained as purple solid in 50% yield. The dyad **2** was prepared by reacting **26** and **29** and dyad **3** was prepared by reacting **27** and **29** under similar click reaction conditions used for dyad **1** and afforded in 46–48% yields (Scheme 3). The free-base dyads **4** and **5** were prepared by demetallation of dyads **1** and **2**, respectively, in CH_2Cl_2 in the presence of small amount of TFA at room temperature. The free-base porphyrin dyad **6** was prepared under same conditions by reacting **26** and **30** in THF/CH_3CN in the presence of CuI/DIPEA at room temperature for 12 h. The N_3S porphyrins are known to form metal complexes which require harsh reaction conditions[12,15] and N_2S_2 porphyrins generally do not form metal complexes although one report on Ru(II) complex of N_2S_2 porphyrin is available in literature.[16] Thus, to synthesize the triazole-bridged free base porphyrin dyads containing two different types of heteroporphyrin sub-units such as compound **6**, the reaction conditions developed for the synthesis of compounds **1**–**3** are applicable. However, the dyads containing free base N_4 porphyrin and heteroporphyrin sub-units can be obtained only through demetallation of the corresponding metallated N_4-heteroporphyrin dyads.

The dyads **1**–**6** were characterized by mass, NMR, absorption, electrochemical and fluorescence techniques. The dyads **1**–**6** showed a peak corresponding to the loss of N_2 in the MALDI-TOF spectra. The ^{1}H NMR resonances of dyads **1**–**6** were assigned on the basis of spectra observed for the corresponding porphyrin monomers taken independently. For example, in dyad **1**, the signals of the two β-thiophene protons appeared as sets of two doublets at δ = 9.79 and 9.84 ppm; the eight β-pyrrole protons of the ZnN_4 porphyrin sub-unit gave rise to three sets of signals in the 8.8–9.1 ppm region; the signals of the six β-pyrrole protons of N_3S porphyrin sub-unit appeared at δ = 8.71–8.74; the triazole signal appeared as singlet at δ = 8.79 and the inner NH signal appeared as singlet at δ = –2.65 ppm. Similarly the dyads **2** and **3** also showed similar features and signals were assigned by comparing them with their corresponding porphyrin monomers. A comparison of chemical shifts of various protons of the dyads **1**–**3** with those of their corresponding individual monomer units indicate only minor differences suggesting that the two porphyrin sub-units in dyads **1**–**3** interact very weakly. The dyads **4** and **5** which were prepared by demetallation of the corresponding dyads **1** and **2** showed similar ^{1}H NMR spectral features like their corresponding metallated dyads and exhibited an additional signal at –2.70 ppm corresponding to two inner NH signals of N_4 porphyrin sub-unit. The free-base dyad **6** containing a N_3S and N_2S_2 porphyrin sub-units showed the combined ^{1}H NMR spectral features of its corresponding N_3S and N_2S_2 porphyrin monomers with negligible changes in their chemical shifts compared to its constituted porphyrin monomers supporting that the two porphyrin sub-units interact very weakly and retain most of their ^{1}HNMR spectral features. Thus, ^{1}H NMR studies indicate that porphyrin sub-units in triazole-bridged porphyrin dyads **1**–**6** interact very weakly and retain most of their individual ^{1}H NMR spectral features.

Absorption, Electrochemical and Fluorescence Properties of Dyads 1–6

The absorption spectra of dyads **1**–**6** along with *meso*-(azidophenyl)porphyrin monomers **24**–**27** were recorded in dichloromethane and data are presented in Table 1. The comparison of absorption spectra of dyad **5** along with its corresponding porphyrin monomers **26** and **28** is shown in Figure 4. According to Figure 4 the absorption spectra of the dyads show the absorption bands corresponding to both the constituted porphyrin monomers. For instance, the dyad **1** containing ZnN_4 and N_3S porphyrin sub-units showed 515, 549, 587, 615 and 677 nm in Q-band region and 422 nm with a shoulder at 430 nm in Soret band region. In this dyad, the bands at 515, 615, 677 and 430 nm were exclusively due to N_3S porphyrin sub-unit and the bands at 549, 587 and 422 nm are majorly due to ZnN_4 porphyrin sub-unit. Similarly in all other dyads, the absorption bands corresponding to both the porphyrin sub-units are present. The comparison of absorption spectra of dyads **1**–**6** with those of their corresponding porphyrin monomers indicate that the absorption bands of dyads are sum of the absorption bands of their corresponding porphyrin monomers with negligible shifts in their peak maxima supporting a very weak interaction among the two porphyrin sub-units in dyads **1**–**6**.

The redox chemistry of the triazole-bridged porphyrin dyads containing two different macrocycles **1**–**6** along with their *meso*-(azidophenyl)porphyrin monomers **24**–**27** was followed by cyclic voltammetry at a scan rate of 50 mV/s and differential pulse voltammetry (DPV) using tetrabutylammonium perchlorate as supporting electrolyte (0.1 M) in dichloromethane. The representative reduction waves of dyads **1** and **5** are presented in Figure 5. In general dyads **1**–**6** showed two or three oxidations and three or four reductions and peak potentials were assigned on the basis of their corresponding *meso*-(azidophenyl)porphyrin monomers. For instance the dyad **1** containing ZnN_4 and N_3S porphyrin sub-units showed three oxidations at 0.77, 1.07 and 1.47 V and three reductions at –1.02, –1.35 and –1.55 V. The first oxidation at 0.77 V was due to oxidation of ZnN_4 porphyrin sub-unit because it is easier to oxidize as compared to free base N_3S porphyrin. The oxidation at 1.47 V was assigned to the oxidation of N_3S porphyrin sub-unit and oxidation at 1.07 V was due to oxidation of both ZnN_4 and N_3S porphyrin sub-units. Similarly, the first reduction at –1.02 V was due to reduction of N_3S porphyrin sub-unit; the last reduction at –1.55 V was due to reduction of ZnN_4 porphyrin sub-unit and reduction at –1.35 V was due to reduction of both ZnN_4 and N_3S porphyrin sub-units. Similarly, the other dyads also exhibited oxidation and reduction waves, and the peak potentials were in the same range of their corresponding porphyrin monomers (Table 1). Thus, the electrochemical studies also indicated that the two porphyrin sub-units in dyads **1**–**6** interact very weakly.

The steady state and time-resolved fluorescence studies of dyads **1**–**6** along with their appropriate reference com-

Table 1. Absorption and electrochemical data of click dyads **1**–**6** along with the (azidophenyl)porphyrin monomers **24**–**27** recorded in dichloromethane.

Compound	Soret band λ [nm] (logε)		Q bands λ [nm] (logε)		Potential (V) vs. SCE					
					Oxidation			Reduction		
24	420 (6.02)		516 (4.56)	552 (4.29)		1.00	1.40	–1.18		–1.54
			591 (3.99)	647 (3.96)						
Zn24	421 (5.36)		548 (4.05)	588 (3.53)	0.78	1.08		–1.26		–1.56
25	430 (5.79)		515 (4.57)	551 (4.11)		1.06	1.43	–1.03		–1.38
			618 (3.54)	678 (3.91)						
26	437 (5.46)		515 (4.38)	550 (3.95)		1.14	1.53	–0.93		–1.26
			634 (2.98)	698 (3.70)						
27	433 (5.05)		513 (4.20)	546 (3.67)		1.07	1.42	–0.95		–1.18
			645 (3.07)	711 (3.65)						
1	422 (5.86)	430 (sh)	515 (4.43)	549 (4.52)	0.77	1.07	1.47	–1.02	–1.35	–1.55
			587 (3.89)	615 (3.61)						
			677 (3.76)							
2	422 (5.69)	437 (5.50)	515 (4.39)	550 (4.39)	0.77	1.06	1.31	–0.83	–1.19	–1.52
			589 (3.73)	633 (3.34)						
			697 (3.71)							
3	422 (5.71)		512 (4.31)	548 (4.34)	0.78	1.08		–0.92	–1.14	–1.58
			588 (3.72)	644 (3.07)						
			710 (3.62)							
4	421 (5.55)	429 (sh)	515 (4.40)	551 (4.10)		1.07	1.45	–1.03	–1.17	–1.34
			591 (3.65)	614 (3.50)						–1.51
5	420 (5.30)	436 (5.14)	515 (4.23)	551 (3.91)		1.05	1.12	1.38	–0.82	–1.12	–1.48
			590 (3.36)	647 (3.37)						
			697 (3.37)							
6	435 (5.35)		515 (4.30)	550 (3.98)		1.08	1.40	1.59	–0.89	–1.02	–1.33
			621 (3.30)	680 (3.50)						
			695 (3.51)							

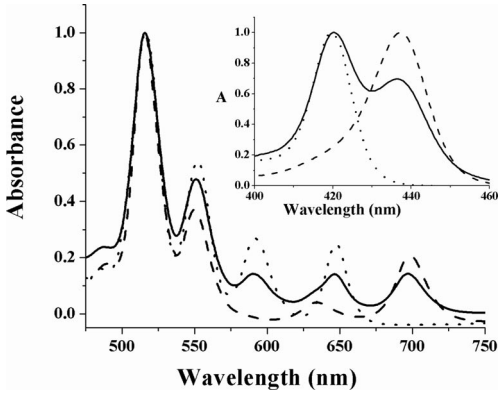

Figure 4. Q-band absorption spectra of **5** (solid line), **28** (dotted line) and **26** (dashed line) recorded in dichloromethane. The inset shows their corresponding Soret band absorption spectra.

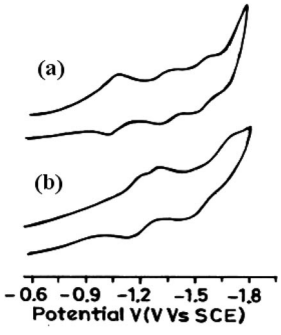

Figure 5. Reduction waves of click dyads (a) **1** and (b) **5** recorded in dichloromethane with TBAP as supporting electrolyte (scan rate: 50 mV/s).

pounds were recorded in dichloromethane at room temperature and the data is presented in Table 2. In dyads **1**–**3**, the ZnN_4 porphyrin sub-unit acts as energy donor and absorbs strongly at 550 nm; N_3S, N_2S_2 and N_2SO porphyrin sub-units respectively acts as energy acceptors and do not absorb strongly at 550 nm. A comparison of steady state emission spectra of ZnN_4–N_3S dyad **1** along with its 1:1 mixture of corresponding porphyrin monomers **25** and **29** recorded at 550 nm is shown in part a of Figure 6. Inspection of this reveals that on excitation of dyad at 550 nm where the ZnN_4 porphyrin sub-unit absorbs strongly, the emission from ZnN_4 porphyrin emission is quenched by 87% and a strong emission is observed from the N_3S porphyrin sub-unit. However, when the 1:1 mixture of its corresponding monomers was recorded at 550 nm, the emission was exclusively observed for the ZnN_4 porphyrin sub-unit. Furthermore, the excitation spectrum of the dyad **1** recorded at 750 nm matched closely with the absorption spectrum. These results indicate that there is an efficient energy transfer in singlet state from the ZnN_4 porphyrin sub-unit to the N_3S porphyrin sub-unit. Similarly, in the case of dyad **2**, upon excitation at 550 nm, the emission from the ZnN_4 porphyrin sub-unit is quenched significantly and a strong emission is observed for the N_2S_2 porphyrin sub-unit, which supports an efficient energy transfer from the ZnN_4 porphyrin sub-unit to the N_2S_2 porphyrin sub-unit in dyad **2**. Interestingly, in the case of dyad **3** containing ZnN_4 and

Table 2. Emission data of click dyads **1**–**6** along with the (azidophenyl)porphyrin monomers **24**–**27** recorded in dichloromethane.

Compound	Φ_{donor}	% Quenching	τ_{donor} [ps]	Energy transfer efficiency
24	0.084	–	8140	–
Zn24	0.036	–	1590	–
25	0.016	–	1590	–
26	0.0073	–	1240	–
27	0.013	–	1030	–
1	0.0046	87	150	90
2	0.0036	90	190	88
3	0.01	73	990	37
4	0.0028	97	230	97
5	0.0014	98	280	97
6	0.0005	–	290	–

N_2SO porphyrin sub-units, the energy transfer is not efficient from the ZnN_4 porphyrin to the N_2SO porphyrin sub-unit. This requires further investigation.

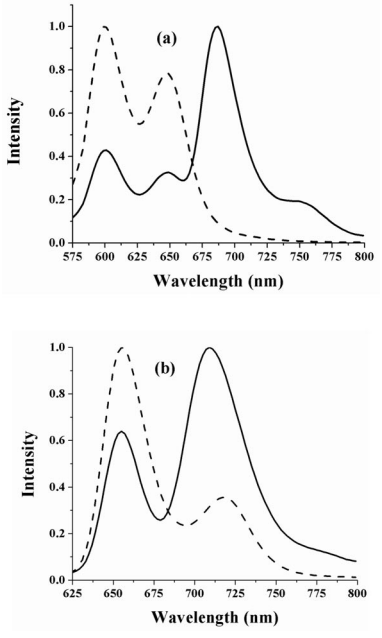

Figure 6. Comparison of emission spectra of click dyads (thick line) (a) **1** and (b) **5** along with 1:1 mixture of corresponding monomers (dashed line) recorded in dichloromethane at λ_{ex} = 550 and 410 nm, respectively.

The steady-state fluorescence spectra of the free-base porphyrin dyads **4** and **5** were recorded at 420 nm where the N_4 porphyrin sub-unit absorbs strongly. As is clear from Figure 6 (b) shown for dyad **5**, on excitation at 420 nm, the emission from the N_4 porphyrin sub-unit was quenched by 98% and the strong emission was noted mainly from N_2S_2 porphyrin sub-unit. Similar observation was made for dyad **4** also, where the N_4 porphyrin sub-unit was quenched by 97% and a strong emission was noted for the N_3S porphyrin sub-unit. These results support an efficient energy transfer in the singlet state from the N_4 porphyrin sub-unit to the heteroporphyrin sub-unit in dyads **4** and **5**. The fluorescence spectrum of free-base dyad **6** containing N_3S and N_2S_2 porphyrin sub-units was recorded at 425 nm where N_3S porphyrin sub-unit absorbs relatively strongly compared to the N_2S_2 porphyrin sub-unit. Although the major emission was noted from the N_2S_2 porphyrin sub-unit, in this case it is difficult to calculate the magnitude of emission of N_3S porphyrin sub-unit quenched because the emission bands of both N_3S and N_2S_2 porphyrin sub-units overlap with each other significantly. However, the fact that the emission was noted mainly from N_2S_2 porphyrin sub-unit, we conclude that the energy transfer is possible from the N_3S porphyrin sub-unit to the N_2S_2 porphyrin sub-unit in dyad **6**.

The time-resolved fluorescence studies carried out on dyads **1**–**6** also support the assumption of an efficient energy transfer from one porphyrin sub-unit to the other in dyads **1**–**6**. The dyads were excited at 406 nm and monitored at two different wavelengths corresponding to the emission peak maxima of donor porphyrin sub-unit and acceptor porphyrin sub-unit. The fluorescence decays of dyads **1**–**6** monitored at acceptor heteroporphyrin sub-unit was fitted to single exponential and the lifetime τ was closely matched with the corresponding porphyrin monomer. The fluorescence decays of dyads **1**–**6** monitored at emission peak maxima of donor porphyrin sub-unit were fitted to two exponential with a dominant contribution from one component. For instance the fluorescence decay of dyad **1** was fitted to two exponential decay with lifetime of 150 ps (90%) as the major component and decay with lifetime of 1.2 ns (10%) as the minor component. The minor component with life time of 1.2 ns was attributed to the monomeric porphyrin impurity present in the dyad **1** and the major component decay with 150 ps is the quenched lifetime of donor ZnN_4 porphyrin sub-unit due to singlet–singlet energy transfer from the donor ZnN_4 porphyrin sub-unit to the acceptor N_3S porphyrin sub-unit. In other dyads **2**–**5**, similar observations were made and the shorter major component decay was attributed to energy transfer from donor porphyrin sub-unit to acceptor porphyrin sub-unit (Table 2).

Triazole-Bridged Porphyrin–Ferrocene Conjugates 7–11

The *meso*-(azidophenyl)porphyrin building blocks **24**–**27** were used further to synthesize triazole-bridged porphyrin–ferrocene conjugates **7**–**11**. Linking ferrocene moieties to porphyrin is of interest because the ferrocene, according to thermodynamic considerations, is able to reduce porphyrin

hence porphyrin–ferrocene hybrid molecules can be used in various photochemical devices, including donor-acceptor molecules that mimic the initial stages in the photosynthetic process at the molecular level.[17] Herein we describe the utility of *meso*-(azidophenyl)porphyrin building blocks for the synthesis of triazole-bridged porphyrin–ferrocene conjugates under similar click reaction condition used above for the synthesis of unsymmetrical porphyrin dyads. In a typical reaction, one equivalent of *meso*-(azidophenyl)porphyrin building block was treated with one equivalent of ethynyl ferrocene in THF/CH_3CN in the presence of CuI/DIPEA at room temperature for 12 h (Scheme 3). TLC analysis showed three spots corresponding to the small amounts of unreacted starting materials as first two spots followed by the major polar spot corresponding to the required porphyrin–ferrocene conjugates. Column chromatographic purification on silica gel afforded pure porphyrin–ferrocene conjuagates **7**–**11** in 48–52% yield. The porphyrin–ferrocene conjugate **8** was obtained in quantitative yield by demetallation of **7** by treating it with TFA in CH_2Cl_2 for 1 h followed by column chromatographic purification. The porphyrin–ferrocene conjugates **7**–**11** were highly soluble in all common organic solvents and characterized by mass, NMR, absorption, electrochemical and fluorescence techniques.

The molecular ion peak in ES-MS mass spectra confirmed the identity of all porphyrin–ferrocene conjugates **7**–**11**. It is clear that the conjugate **9** exhibits similar NMR features like *meso*-(azidophenyl)porphyrin monomer **25** except for a few changes. The 2, 6-protons of *meso*-phenyl group which is connected to the triazole ring was shifted downfield by about 1 ppm; a characteristic singlet at 8.2 ppm for the triazole proton and three signals in 4.2–5.1 ppm region for nine ferrocene proton signals. In the remaining conjugates, apart from the above-mentioned changes, we also noticed the presence of minor sets of additional signals for ferrocenyl as well as for selected porphyrinic protons which may be arising from the dynamic processes such as rotational isomerism taking place in solution at room temperature.[18] In general the chemical shift patterns of all conjugates were almost matching with those of corresponding *meso*-(azidophenyl)porphyrins supporting weak interaction between porphyrin and ferrocenyl subunits.

The absorption spectra of conjugates **7**–**11** were recorded in dichloromethane. The absorption peak maxima of conjugates are exactly matching with their corresponding *meso*-(azidophenyl)porphyrin monomers with slight alterations in their extinction coefficients supporting a weak interaction between porphyrin and ferrocene sub-units (Table 3). The electrochemical properties of porphyrin–ferrocene conjugates **7**–**11** were followed by cyclic voltammetry at scan rate of 50 mV/s using tetrabutylammonium perchlorate as supporting electrolyte in dichloromethane. In general, as mentioned above, the porphyrins exhibit two oxidation and two reduction waves corresponding to the formation of mono, dications and mono, dianions of porphyrin ring respectively.[19] The absolute $E_{1/2}$ values depend on the nature of the porphyrin. In porphyrin–ferrocene conjugates, an additional redox couple corresponding to the oxidation of ferrocene ring is also expected. A comparison of oxidation and reduction waves of *meso*-(azidophenyl)porphyrin **25** and azidoporphyrin–ferrocene conjugate **9** is shown in Figure 7 and the data is presented in Table 3. The ethynyl ferrocene shows a reversible oxidation couple at 0.65 V.[17] In triazole-bridged porphyrin–ferrocene conjugates **7**–**11**, the reversible oxidation couple was noted in 0.53–0.57 V region. Thus, in conjugates **7**–**11**, the ferrocene group is easier to oxidize which can be rationalized as follows. In porphyrin–ferrocene conjugate, the *meso*-phenyl groups are orthogonal to the porphyrin plane thus preventing the electron density distribution between porphyrin and ferrocene groups resulting in easier oxidation of ferrocene ring compared to ethynyl ferrocene. The oxidation and reduction potentials of

Table 3. Absorption and electrochemical data of porphyrin–ferrocene click conjugates **7**–**11** recorded in dichloromethane.

Compound	Soret band	Q-bands	Potential [V] vs. SCE				
	λ [nm] (log ε)	λ [nm] (log ε)	Oxidation			Reduction	
			I	II	III	I	II
7	421 (5.81)	548 (4.39) 587 (3.65)	0.57	0.79	1.10	–1.50	–1.70
8	419 (5.84)	516 (5.84) 551 (4.15) 591 (3.84) 647 (3.76)	0.57	1.03	1.47	–1.17	–1.49
9	430 (5.47)	515 (4.34) 550 (3.87) 617 (3.28) 677 (3.66)	0.53	1.08		–1.04	–1.36
10	437 (5.57)	515 (4.50) 549 (4.04) 634 (3.02) 697 (3.79)	0.56			–0.89	–1.20
11	433 (5.13)	513 (4.24) 544 (3.62) 645 (2.67) 711 (3.61)	0.57	1.13		–0.93	–1.18

Table 4. Emission data of porphyrin–ferrocene click conjugates **7**–**11** recorded in dichloromethane.

Compound	λ_{em} [nm]		Φ_f	τ_f [ns]	k_{rad} [10^6 s^{-1}]	k_{nr} [10^8 s^{-1}]
7	600	648	0.029	1.11	26.12	8.74
8	653		0.032	4.35	7.35	2.22
9	686		0.0091	1.11	8.19	8.92
10	709		0.0040	1.16	3.44	8.58
11	718		0.0065	0.81	8.02	12.26

porphyrin ring did not show any shifts compared to *meso*-(azidophenyl)porphyrins further supporting a weak interaction between ferrocene and porphyrin sub-units in porphyrin–ferrocene conjugates **7**–**11**. The fluorescence properties of porphyrin–ferrocene conjugates **7**–**11** were studied by both steady state and time-resolved fluorescence techniques. The comparison of steady state fluorescence spectra of porphyrin–ferrocene conjugate **9** with *meso*-(azidophenyl)porphyrin **25** is shown in Figure 8 and the data are tabulated in Table 4. Inspection of Figure 8 and Table 4 indicates that the emission peak maxima of porphyrin in porphyrin–ferrocene conjugates is almost identical with the emission peak maxima of the corresponding monomeric porphyrin. However, the quantum yields of porphyrin in porphyrin–ferrocene conjugates are decreased compared to the corresponding monomeric porphyrins. The singlet state lifetime for porphyrin–ferrocene conjugates was measured by single-photon counting technique. All conjugates were excited at 406 nm and were detected at the emission peak maxima of the porphyrin in porphyrin–ferrocene conjugates. The fluorescence decays of porphyrin–ferrocene conjugates **7**–**11** were fitted to single exponential decay functions. The singlet state lifetime τ, rate of radiative decay k_r and rate of nonradiative decay k_{nr} presented in Table 4 reveal the following as compared to their corresponding reference *meso*-(azidophenyl)porphyrin monomers: (1) the singlet state lifetime τ of porphyrin in porphyrin–ferrocene conjugates **7**–**11** is decreased. (2) The rates of radiative decay k_r is decreased and non-radiative decay k_{nr} is increased for porphyrin in porphyrin–ferrocene conjugates **7**–**11**. All these results suggest that the fluorescence of porphyrin in porphyrin–ferrocene conjugates is significantly quenched which is attributed tentatively to electron transfer from ferrocene to singlet excited state of porphyrin.

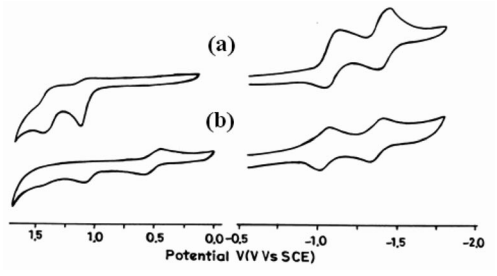

Figure 7. Cyclic voltammogram of (a) **25** and (b) **9** recorded in dichloromethane with TBAP as supporting electrolyte (scan rate: 50 mV/s).

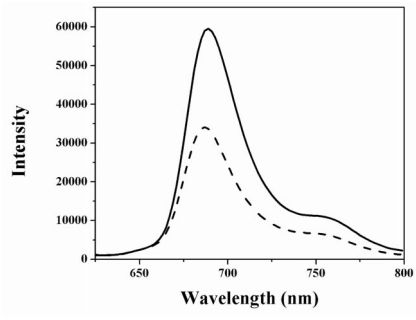

Figure 8. Comparison of emission spectra of **25** (solid line) and **9** (dotted line) recorded in dichloromethane. The concentration used was 2×10^{-6} M.

Conclusions

Three new mono-nitroporphyrins with N_3S, N_2S_2 and N_2SO cores were synthesized by condensing an unsymmetrical thiophenediol with *p*-tolualdehyde/pyrrole, 16-thiatripyrrin and 16-oxatripyrrin, respectively, under mild porphyrin-forming conditions. The mono-aminoporphyrins were synthesized from corresponding mono-nitroporphyrins under standard $SnCl_2$/HCl conditions. The mono-azidoporphyrins were synthesized by adopting a simple approach of treating mono-aminoporphyrins with *tert*-butyl nitrite/azidotrimethylsilane at room temperature. The mono-azidoporphyrins have been used to synthesize a series of triazole-bridged unsymmetrical porphyrin dyads containing two different porphyrin sub-units and triazole-bridged porphyrin–ferrocene conjugates under "click reaction" conditions. Under various Cu^I-catalyzed click reaction conditions employed, the best yields were obtained when we used CuI/DIPEA (0.1:1) in THF/CH_3CN at room temperature for overnight. The ground state properties of dyads and conjugates indicate a weak interaction between the two sub-units. A preliminary photophysical studies support an efficient energy transfer from one porphyrin sub-unit to another in unsymmetrical porphyrin dyads and electron-transfer from ferrocene to porphyrin in porphyrin–ferrocene conjugates. Presently, we are exploring the click reaction approach developed in this paper to synthesize more elaborate assemblies.

Experimental Section

Chemicals: All general chemicals and solvents were procured from S.D. Fine chemicals, India. Column chromatography was performed using silica gel and basic alumina obtained from Sisco Re-

search Laboratories, India. *tert*-butyl nitrite and Azidotrimethylsilane were purchased from Aldrich. Tetrabutylammonium perchlorate was purchased from Fluka and used without further purifications.

Instrumentation: ^{1}H NMR spectra were recorded with Varian 300 and 400 MHz instruments using tetramethylsilane (TMS) as an internal standard. ^{13}C NMR spectra were recorded on Varian spectrometer operating at 100.6 MHz. All NMR measurements were carried out at room temperature in deuteriochloroform ($CDCl_3$). Absorption and steady state fluorescence spectra were obtained with Perkin–Elmer Lambda-35 and PC1 Photon Counting Spectrofluorometer manufactured by ISS USA, respectively. The fluorescence quantum yields (Φ_f) were estimated from the emission and absorption spectra by comparative method.[20] The time-resolved fluorescence decay measurements[21] were carried out at magic angle using a picosecond diode laser based time correlated single photon counting (TCSPC) fluorescence spectrometer from IBH, UK. The energy transfer efficiencies for dyads **1**–**5** were calculated from the lifetime data of dyads and their corresponding appropriate monomers.[20] The radiative and non-radiative rate constants, k_r and k_{nr} were calculated by the following equations:

$$\Sigma K = 1/\tau_f \quad (1)$$

$$k_r = \Phi_f k \quad (2)$$

$$k_{nr} = k - k_r \quad (3)$$

ES-MS spectra were recorded with a Q-Tof Micromass spectrometer. MALDI-TOF spectra were obtained from Axima-CFR manufactured by Kratos Analyticals. Cyclic voltammetric (CV) and differential pulse voltammetric (DPV) studies were carried out with BAS electrochemical system utilizing the three electrode configuration consisting of a glassy carbon (working electrode), platinum wire (auxiliary electrode) and saturated calomel (reference electrode) electrodes in dry dichloromethane using 0.1 M tetrabutylammonium perchlorate as supporting electrolyte.

5-(4-Nitrophenyl)-10,15,20-tri(*p*-tolyl)porphyrin (12): Samples of *p*-tolualdehyde (1.19 g, 1.17 mL, 9.9 mmol), 4-nitrobenzaldehyde (0.5 g, 3.3 mmol) and pyrrole (0.87 g, 0.91 mL, 13.2 mmol) were dissolved in dichloromethane (300 mL) and purged with nitrogen whilst stirring for 10 min. The condensation was initiated by adding catalytic amount of $BF_3{\cdot}OEt_2$ (0.4 mL of 2.5 M solution) and stirring was continued for 1 h under nitrogen atmosphere at room temperature. 2,3-Dichloro-5,6-dicyano-benzoquinone (DDQ) (0.75 g, 3.3 mmol) was then added and the reaction mixture was stirred in air for additional 1 h. The solvent was removed under reduced pressure and the crude compound was subjected to silica gel column chromatography. The desired compound was moved as purple band with petroleum ether/dichloromethane (60:40) and the solvent was removed on rotary evaporator to afford pure nitro porphyrin in 10% yield (232 mg); m.p. >300 °C. ^{1}H NMR (400 MHz, $CDCl_3$): δ = –2.77 (s, 2 H, NH), 2.70 (s, 9 H, CH_3), 7.55 (d, J = 7.7 Hz, 6 H, Ar), 8.08 (d, J = 7.7 Hz, 6 H, Ar), 8.37 (d, J = 8.2 Hz, 2 H, Ar), 8.61 (d, J = 8.7 Hz, 2 H, Ar), 8.70 (d, J = 5.0 Hz, 2 H, β-pyrrole), 8.80 (s, 4 H, β-pyrrole), 8.89 (d, J = 4.5 Hz, 2 H, β-pyrrole) ppm. ^{13}C NMR (100 MHz, $CDCl_3$): δ = 21.2, 116.5, 120.8, 121.3, 121.8, 127.0, 128.2, 134.0, 134.8, 135.3, 137.7, 139.2, 147.8, 149.5 ppm. ES MS: *m*/*z* (%) = 702.33 (100) $[M]^+$. $C_{47}H_{35}N_5O_2$ (701.81): calcd. C 80.43, H 5.03, N 9.98; found C 80.50, H 4.98, N 10.01. UV/Vis [in dichloromethane, λ_{max}/nm (log ε)]: 420 (5.57), 516 (4.23), 553 (3.98), 591 (3.74), 647 (3.67).

2-[Hydroxy(4-nitrophenyl)methyl]-5-[hydroxy(*p*-tolyl)methyl]thiophene (14): *N*,*N*,*N*′,*N*′-Tetramethyl ethylenediamine (1.9 mL, 12.2 mmol) and *n*BuLi (7.70 mL of 1.6 M solution in hexane, 12.2 mmol) were added to a solution of 2-(*p*-tolylhydroxymethyl)-thiophene (**13**) (1 g, 4.9 mmol) in diethyl ether (30 mL) and stirred at 0 °C for 1 h. An ice cold solution of 4-nitrobenzaldehyde (0.9 g, 5.8 mmol) in THF was added and stirring was continued for an additional 1 h. Saturated aqueous NH_4Cl solution was added to the reaction mixture and was extracted with diethyl ether (3 × 50 mL). The organic layers were combined, washed with saturated brine and dried with sodium sulfate. The crude product was concentrated in vacuo and purified by silica gel column chromatography using petroleum ether/ethyl acetate (72:28) to afford the diol **14** as white solid in 47% yield (800 mg); m.p. 125 °C. ^{1}H NMR (400 MHz, $CDCl_3$): δ = 2.34 (s, 3 H, tolyl), 2.43 (br. s, 1 H, OH), 2.65 (br. s, 1 H, OH), 5.92 (s, 1 H, CHOH), 6.06 (s, 1 H, CHOH), 6.70 (d, J = 3.3 Hz, 1 H, thiophene), 6.75 (d, J = 3.3 Hz, 1 H, thiophene), 7.16 (d, J = 7.9 Hz, 2 H, Ar), 7.29 (d, J = 8.2 Hz, 2 H, Ar), 7.60 (d, J = 9.1 Hz, 2 H, Ar), 8.19 (d, J = 8.8 Hz, 2 H, Ar) ppm. ^{13}C NMR (100 MHz, $CDCl_3$): δ = 21.3, 71.6, 72.6, 110.2 123.9, 124.5, 125.3, 126.3, 127.1, 129.5, 138.2, 139.9, 146.4, 149.7, 149.8 ppm. ES MS: *m*/*z* (%) = 338.07 (100) [M – OH]$^+$. $C_{19}H_{17}NO_4S$ (355.41): calcd. C 64.21, H 4.82, N 3.94, S 9.02; found C 64.25, H 4.75, N 3.95, S 9.05.

5-(4-Nitrophenyl)-10,15,20-tri(*p*-tolyl)-21-thiaporphyrin (15): Samples of **14** (0.5 g, 1.4 mmol), *p*-tolualdehyde (0.33 mL, 2.8 mmol) and pyrrole (0.29 mL, 4.2 mmol), were dissolved in dichloromethane (300 mL) degassed with nitrogen and stirred for 10 min. The condensation was initiated by adding $BF_3{\cdot}OEt_2$ (0.4 mL of 2.5 M solution) while stirring the reaction mixture at room temperature for 1 h under nitrogen atmosphere. DDQ (0.32 g, 1.4 mmol) was then added and the reaction mixture was stirred in air for additional 1 h. The crude compound containing mixture of porphyrins was subjected to silica gel column chromatography using petroleum ether/dichloromethane (60:40) which afforded monothia nitro porphyrin **15** in 8% yield (80 mg); m.p. >300 °C. ^{1}H NMR (400 MHz, $CDCl_3$): δ = –2.68 (s, 2 H, NH), 2.70 (s, 9 H, CH_3), 7.52 (d, J = 7.6 Hz, 4 H, Ar), 7.62 (d, J = 7.9 Hz, 2 H, Ar), 8.06 (d, J = 7.9 Hz, 4 H, Ar), 8.12 (d, J = 7.9 Hz, 2 H, Ar), 8.40 (d, J = 8.5 Hz, 2 H, Ar), 8.56 (d, J = 4.2 Hz, 1 H, β-pyrrole), 8.62 (d, J = 4.2 Hz, 1 H, β-pyrrole) 8.65–8.68 (m, 4 H, Ar) 8.96 (m, 2 H, β-pyrrole) 9.60 (d, J = 5.1 Hz, 1 H, β-thiophene) 9.78 (d, J = 5.1 Hz, 1 H, β-thiophene) ppm. ^{13}C NMR (100 MHz, $CDCl_3$): δ = 22.0, 123.1, 125.01125.5, 127.9, 128.9, 129.6, 129.8, 132.5, 132.8, 133.4, 133.7, 134.7, 134.9, 135.2, 135.5, 136.3, 136.7, 138.2, 138.3, 139.8, 139.9, 140.0, 147.2, 147.3, 148.2, 148.6, 155.2, 156.7, 158.4 ppm. ES MS: *m*/*z* (%) = 718.85 (100) $[M]^+$. $C_{47}H_{34}N_4O_2S$ (718.86): calcd. C 78.53, H 4.77, N 7.79, S 4.46; found C 78.60, H 4.70, N 7.83, S 4.48. UV/Vis [in dichloromethane, λ_{max}/nm (log ε)]: 431 (5.48), 516 (4.36), 553 (3.97), 617 (3.57), 676 (3.73).

5-(4-Nitrophenyl)-10,15,20-tri(*p*-tolyl)-21,23-dithiaporphyrin (17): A solution of **14** (0.5 g, 1.4 mmol) and 5,10-bis(*p*-tolyl)-15,17-dihydro-16-thiatripyrrane (0.6 g, 1.4 mmol) in dichloromethane (300 mL) was degassed with nitrogen whilst stirring for 10 min. $BF_3{\cdot}OEt_2$ (0.4 mL of 2.5 M solution) was added to initiate the condensation and the reaction mixture was stirred at room temperature for 1 h under nitrogen atmosphere. DDQ (0.32 g, 1.4 mmol) was added and the reaction mixture was stirred in air for additional 1 h. The solvent was removed under reduced pressure and the tlc analysis of crude compound showed the formation of desired compound as sole product. The crude compound was subjected to silica gel column chromatography using petroleum ether/dichloromethane (60:40) to obtain the pure mononitrodithiaporphyrin **17** in 10% yield (103 mg); m.p. >300 °C. ^{1}H NMR (400 MHz, $CDCl_3$): δ = 2.70 (s, 9 H, CH_3), 7.61 (d, J = 7.6 Hz, 6 H, Ar), 8.10–8.13 (m, 6

H, Ar), 8.37 (d, J = 8.8 Hz, 2 H, Ar), 8.54 (d, J = 4.5 Hz, 1 H, β-pyrrole), 8.64–8.69 (m, 4 H, β-pyrrole + Ar), 8.72 (d, J = 4.5 Hz, 1 H, β-pyrrole) 9.52 (d, J = 5.1 Hz, 1 H, β-thiophene), 9.72 (d, J = 4.5 Hz, 3 H, β-thiophene) ppm. ^{13}C NMR (100 MHz, $CDCl_3$): δ = 21.6, 122.7, 128.4, 130.0, 133.5, 134.1, 134.3, 134.7, 134.8, 134.9, 135.0, 135.2, 135.4, 135.8, 136.0, 136.2, 138.1, 138.2, 138.3, 147.1, 147.6, 147.9, 148.2, 148.3, 148.6, 148.6, 155.3, 156.7, 156.8, 157.0 ppm. ES MS: m/z (%) = 736.2 (100) $[M]^+$. $C_{47}H_{33}N_3O_2S_2$ (735.91): calcd. C 76.71, H 4.52, N 5.71, S 8.71; found C 76.61, H 4.57, N 5.77, S 8.75. UV/Vis [in dichloromethane, λ_{max}/nm ($\log\varepsilon$)]: 438 (5.65), 516 (4.66), 551 (4.28), 634 (3.68), 698 (4.03).

5-(4-Nitrophenyl)-10,15,20-tri(*p*-tolyl)-21-thia-23-oxaporphyrin (19): The samples of **14** (0.5 g, 1.4 mmol) and 5,10-bis(*p*-tolyl)-16-oxa-15,17-dihydrotripyrrane (**18**) were condensed in dichloromethane (300 mL) in the presence of catalytic amount of $BF_3{\cdot}OEt_2$ (0.4 mL of 2.5 M solution) for 1 h under nitrogen atmosphere followed by oxidation with DDQ at room temperature in air and gave a crude product which was subjected to silica gel column chromatography using dichloromethane/methanol (98:2) to afford **19** in 8% yield (81 mg); m.p. >300 °C. ^{1}H NMR (400 MHz, $CDCl_3$): δ = 2.70 (s, 9 H, CH_3), 7.54 (d, J = 7.6 Hz, 4 H, Ar), 7.61 (d, J = 7.6 Hz, 2 H, Ar), 8.02–8.06 (m, 4 H, Ar), 8.10 (d, J = 8.0 Hz, 2 H, Ar), 8.37–8.47 (m, 5 H, β-pyrrole + Ar), 8.55 (d, J = 4.3 Hz, 1 H, β-pyrrole), 8.66 (d, J = 8.7 Hz, 2 H, Ar), 9.20 (s, 2 H, β-furan), 9.56 (d, J = 5.1 Hz, 1 H, β-thiophene), 9.74 (d, J = 5.1 Hz, 1 H, β-thiophene) ppm. ^{13}C NMR (100 MHz, $CDCl_3$): δ = 21.4, 21.5, 121.2, 121.7, 127.5, 127.6, 129.8, 130.1, 132.4, 133.6, 133.9, 134.1, 134.2, 134.7, 135.8, 136.5, 136.9, 137.5, 137.8, 138.0, 139.3, 139.4, 147.6, 150.1, 150.6, 155.4, 155.6, 156.6, 156.9, 157.8, 159.5 ppm. ES MS: m/z (%) = 720.21 (100) $[M]^+$. $C_{47}H_{33}N_3O_3S$ (719.85): calcd. C 78.42, H 4.62, N 5.84, S 4.45; found C 78.47, H 4.58, N 5.77, S 4.53. UV/Vis [in dichloromethane, λ_{max}/nm ($\log\varepsilon$)]: 432 (5.48), 513 (4.58), 546 (4.06), 644 (3.44), 710 (3.99).

General Synthesis of *meso*-(Aminophenyl)porphyrins 20–23: To a solution of nitroporphyrin in $CHCl_3$/HOAc (1:2) was added a solution of $SnCl_2{\cdot}2H_2O$ (4 equiv.) in concd. aqueous HCl. The mixture was vigorously stirred in a preheated oil bath (65–70 °C) for 30 min, refluxed overnight and neutralized with ammonia solution (25%) to pH 8–9. Chloroform (50 mL) was added, and the mixture was stirred for 1 h. The organic phase was separated, and the water phase was extracted with $CHCl_3$ (2 × 50 mL). The combined organic layer was washed once with dilute ammonia solution, three times with water, dried with anhydrous Na_2SO_4 and then concentrated to dryness. The residue was purified by silica gel column chromatography using petroleum ether/dichloromethane to get pure *meso*-(aminophenyl)porphyrin in 75–84% yield.

5-(4-Aminophenyl)-10,15,20-tri(*p*-tolyl)porphyrin (20): Yield 84%; m.p. >300 °C. ^{1}H NMR (400 MHz, $CDCl_3$): δ = –2.76 (s, 2 H, NH), 2.70 (s, 9 H, CH_3), 3.98 (broad, 2 H, NH_2), 7.05 (d, J = 8.2 Hz, 2 H, Ar), 7.54 (d, J = 8.2 Hz, 6 H, Ar), 7.98 (d, J = 8.2 Hz, 2 H, Ar), 8.09 (d, J = 8.2 Hz, 6 H, Ar), 8.84 (s, 6 H, β-pyrrole), 8.91 (d, J = 4.5 Hz, 2 H, β-pyrrole) ppm. ^{13}C NMR (100 MHz, $CDCl_3$): δ = 21.7, 113.6, 120.1, 127.5, 134.7, 135.8, 137.4, 139.5, 146.1 ppm. ES MS: m/z (%) = 672.38 (100) $[M]^+$. $C_{47}H_{37}N_5$ (671.83): calcd. C 84.02, H 5.55, N 10.42; found C 84.10, H 5.60, N 10.32. UV/Vis [in dichloromethane, λ_{max}/nm ($\log\varepsilon$)]: 421 (5.64), 517 (4.24), 555 (4.06), 593 (3.76), 647 (3.77).

5-(4-Aminophenyl)-10,15,20-tri(*p*-tolyl)-21-thiaporphyrin (21): Yield 75%; m.p. >300 °C. ^{1}H NMR (400 MHz, $CDCl_3$): δ = –2.66 (s, 2 H, NH), 2.70 (s, 9 H, CH_3), 4.02 (broad s, 2 H, NH_2), 7.11 (d, J = 8.2 Hz, 2 H, Ar), 7.53 (d, J = 7.9 Hz, 4 H, Ar), 7.61 (d, J = 7.9 Hz, 2 H, Ar), 8.03–8.08 (m, 6 H, Ar), 8.13 (d, J = 7.9 Hz, 2 H, Ar), 8.60 (d, J = 4.5 Hz, 2 H, β-pyrrole), 8.68 (d, J = 4.5 Hz, 1 H, β-pyrrole) 8.73 (d, J = 4.5 Hz, 1 H, β-pyrrole), 8.92 (m, 2 H, β-pyrrole), 9.74 (d, J = 5.1 Hz, 1 H, β-thiophene), 9.80 (d, J = 5.1 Hz, 1 H, β-thiophene) ppm. ^{13}C NMR (100 MHz, $CDCl_3$): δ = 21.6, 110.1, 114.4, 123.5, 123.8, 127.4, 128.4, 128.8, 128.9, 131.3, 131.5, 132.1, 133.1, 134.2, 134.5, 135.4, 137.6, 138.4, 139.1, 139.8, 146.3, 147.4, 154.5, 154.6, 157.4, 157.9 ppm. ES MS: m/z (%) = 688.80 (100) $[M]^+$. $C_{47}H_{36}N_4S$ (688.88): calcd. C 81.94, H 5.27, N 8.13, S 4.65; found C 81.97, H 5.25, N 8.20, S 4.55. UV/Vis [in dichloromethane, λ_{max}/nm ($\log\varepsilon$)]: 433 (5.72), 517 (4.62), 555 (4.36), 621 (3.82), 682 (4.14).

5-(4-Aminophenyl)-10,15,20-tri(*p*-tolyl)-21,23-dithiaporphyrin (22): Yield 75%; m.p. >300 °C. ^{1}H NMR (400 MHz, $CDCl_3$): δ = 2.70 (s, 9 H, CH_3), 4.04 (broad s, 2 H, NH_2), 7.10 (d, J = 8.2 Hz, 2 H, Ar), 7.60 (d, J = 7.6 Hz, 6 H, Ar), 8.03 (d, J = 4.5 Hz, 2 H, β-pyrrole), 8.12 (d, J = 7.9 Hz, 6 H, Ar), 8.62–8.68 (m, 3 H, Ar + β-pyrrole), 8.73 (d, J = 4.5 Hz, 1 H, β-pyrrole), 9.67–9.72 (m, 3 H, β-thiophene), 9.74 (d, J = 4.8 Hz, 1 H, β-thiophene) ppm. ^{13}C NMR (100 MHz, $CDCl_3$): δ = 21.6, 114.3, 128.3, 131.7, 133.8, 134.0, 134.3, 134.4, 134.5, 134.6, 134.8, 135.3, 135.4, 135.6, 135.7, 137.8, 138.6, 146.5, 147.7, 148.1, 148.2, 156.4, 156.5, 156.6, 156.9 ppm. ES MS: m/z (%) = 706.4 (100) $[M]^+$. $C_{47}H_{35}N_3S_2$ (705.93): calcd. C 79.97, H 5.00, N 5.95, S 9.08; found C 79.95, H 5.05, N 5.92, S 9.10. UV/Vis [in dichloromethane, λ_{max}/nm ($\log\varepsilon$)]: 440 (5.58), 518 (4.56), 555 (4.30), 637 (3.52), 703 (4.04).

5-(4-Aminophenyl)-10,15,20-tri(*p*-tolyl)-21-thia-23-oxaporphyrin (23): Yield 75%; m.p. >300 °C ^{1}H NMR (400 MHz, $CDCl_3$): δ = 2.69 (s, 9 H, CH_3), 3.62 (br. s, 2 H, NH_2), 7.12 (d, J = 8.5 Hz, 2 H, Ar), 7.52 (d, J = 7.6 Hz, 4 H, Ar), 7.60 (d, J = 7.6 Hz, 2 H, Ar), 8.02–8.05 (m, 6 H, Ar), 8.11 (d, J = 7.9 Hz, 2 H, Ar), 8.37–8.38 (m, 2 H, β-pyrrole), 8.53 (d, J = 4.5 Hz, 1 H, β-pyrrole), 8.58 (d, J = 4.5 Hz, 1 H, β-pyrrole), 9.13 (s, 2 H, β-furan), 9.68 (d, J = 5.1 Hz, 1 H, β-thiophene), 9.74 (d, J = 5.1 Hz, 1 H, β-thiophene) ppm. ^{13}C NMR (100 MHz, $CDCl_3$): δ = 21.4, 21.5, 114.2, 120.1, 120.4, 127.5, 128.2, 129.3, 129.5, 131.0, 133.4, 133.5, 133.8, 134.1, 134.3, 134.6, 134.9, 135.1, 135.7, 135.9, 137.5, 137.7, 137.9, 139.7, 146.3, 150.8, 151.0, 155.1, 155.4, 156.3, 156.5, 158.7, 159.1 ppm. MALDI-TOF: m/z (%) = 690.4 (100) $[M]^+$. $C_{47}H_{35}N_3OS$ (689.87): calcd. C 81.83, H 5.11, N 6.09, S 4.65; found C 81.85, H 5.09, N 6.15, S 4.60. UV/Vis [in dichloromethane, λ_{max}/nm ($\log\varepsilon$)]: 435 (5.50), 515 (4.62), 551 (4.24), 648 (3.54), 716 (4.16).

General Synthesis of *meso*-(Azidophenyl)porphyrins 24–27: Sample of *meso*-(aminophenyl)porphyrin was dissolved in CH_3CN /THF (1:1) in a 25 mL round-bottomed flask and cooled to 0 °C in an ice bath. To this stirred mixture was added *t*BuONO (1.5 equiv.) followed by $TMSN_3$ (1.2 equiv.) slowly. The resulting solution was stirred at room temperature for 1 h. The reaction mixture was concentrated under vacuum and the crude product was purified by silica gel chromatography using petroleum ether/dichloromethane to afford pure *meso*-(azidophenyl)porphyrin in 60–90% yield.

5-(4-Azidophenyl)-10,15,20-tri(*p*-tolyl)porphyrin (24): Yield 90%; m.p. >300 °C. ^{1}H NMR (400 MHz, $CDCl_3$): δ = –2.78 (s, 2 H, NH), 2.70 (s, 9 H, CH_3), 7.41 (d, J = 8.2 Hz, 2 H, Ar), 7.55 (d, J = 7.9 Hz, 6 H, Ar), 8.07 (d, J = 7.9 Hz, 6 H, Ar), 8.19 (d, J = 8.2 Hz, 2 H, Ar), 8.80 (d, J = 4.5 Hz, 2 H, β-pyrrole), 8.86 (m, 6 H, β-pyrrole) ppm. ^{13}C NMR (100 MHz, $CDCl_3$): δ = 21.7, 117.5, 120.4, 120.6, 127.6, 131.5, 134.7, 135.8, 137.5, 139.2, 139.3, 139.9 ppm. ES MS: m/z (%) = 698.41 (100) $[M]^+$. $C_{47}H_{35}N_7$ (697.83): calcd. C 80.89, H 5.06, N 14.05; found C 80.95, H 5.09, N 14.12.

5-(4-Azidophenyl)-10,15,20-tri(*p*-tolyl)-21-thiaporphyrin (25): Yield 80%; m.p. >300 °C. ^{1}H NMR (400 MHz, $CDCl_3$): δ = –2.68 (s, 2

H, NH), 2.71 (s, 9 H, CH_3), 7.49 (d, J = 8.5 Hz, 2 H, Ar), 7.55 (d, J = 7.9 Hz, 4 H, Ar), 7.63 (d, J = 7.6 Hz, 2 H, Ar), 8.08 (d, J = 7.6 Hz, 4 H, Ar), 8.12 (d, J = 7.6 Hz, 2H Ar), 8.24 (d, J = 7.6 Hz, 2 H, Ar), 8.62–8.69 (m, 3 H, β-pyrrole), 8.69 (d, J = 4.5 Hz, ^{1}H β-pyrrole), 8.95 (m, 2 H, β-pyrrole), 9.70 (d, J = 5.1 Hz, 1 H, β-thiophene), 9.77 (d, J = 5.1 Hz, 1 H, β-thiophene) ppm. ^{13}C NMR (100 MHz, $CDCl_3$): δ = 21.6, 118.4, 118.7, 124.1, 127.5, 128.4, 129.0, 131.8, 132.7, 133.2, 133.8, 134.3, 134.5, 135.5, 135.6, 135.8, 137.7, 138.0, 139.3, 139.6, 140.1, 147.2, 154.6, 157.2, 157.7 ppm. ES MS: m/z (%) = 685.38 (100) $[M - 28]^+$. $C_{47}H_{34}N_6S$ (714.88): calcd. C 78.96, H 4.79, N 11.76, S 4.49; found C 78.90, H 4.85, N 11.80, S 4.53.

5-(4-Azidophenyl)-10,15,20-tri(*p*-tolyl)-21,23-dithiaporphyrin (26): Yield 80%; m.p. >300 °C. ^{1}H NMR (400 MHz, $CDCl_3$): δ = 2.71 (s, 9 H, CH_3), 7.48 (d, J = 8.5 Hz, 2 H, Ar), 7.62 (d, J = 8.2 Hz, 6 H, Ar), 8.13 (d, J = 7.9 Hz, 6 H, Ar), 8.23 (d, J = 8.5 Hz, 2 H, Ar), 8.64 (d, J = 4.2 Hz, 1 H, β-pyrrole), 8.69–8.71 (m, 3 H, β-pyrrole), 9.63 (d, J = 5.1 Hz, 1 H, β-thiophene), 9.70–9.71 (m, 3 H, β-thiophene) ppm. ^{13}C NMR (100 MHz, $CDCl_3$): δ = 21.6, 118.3, 128.3, 132.5, 134.1, 134.3, 134.5, 134.6, 134.7, 134.8, 134.9, 135.5, 135.6, 135.7, 137.9, 138.2, 138.4, 140.3, 147.8, 147.9, 148.1, 156.3, 156.6, 156.7 ppm. ES MS: m/z (%) = 732.18 (100) $[M]^+$. $C_{47}H_{33}N_5S_2$ (731.93): calcd. C 77.13, H 4.54, N 9.57, S 8.76; found C 77.16, H 4.51, N 9.60, S 8.70.

5-(4-Azidophenyl)-10,15,20-tri(*p*-tolyl)-21-thia-23-oxaporphyrin (27): Yield 60%; m.p. >300 °C. ^{1}H NMR (400 MHz, $CDCl_3$): δ = 2.70 (s, 9 H, CH_3), 7.48 (d, J = 8.2 Hz 2 H, Ar), 7.54 (d, J = 8.2 Hz, 4 H, Ar), 7.61 (d, J = 7.6 Hz, 2 H, Ar), 8.04 (d, J = 7.9 Hz, 4 H, Ar), 8.10 (d, J = 7.9 Hz, 2 H, Ar), 8.21 (d, J = 8.5 Hz, 2 H, Ar), 8.41 (m, 2 H, β-pyrrole), 8.50 (d, J = 4.5 Hz, 1 H, β-pyrrole), 8.55 (d, J = 4.5 Hz, 1 H, β-pyrrole), 9.18 (s, 2 H, β-furan), 9.64 (d, J = 5.1 Hz, 1 H, β-thiophene), 9.72 (d, J = 4.8 Hz, 1 H, β-thiophene) ppm. ^{13}C NMR (100 MHz, $CDCl_3$): δ = 21.7, 118.4, 121.1, 127.7, 128.5, 129.9, 133.2, 133.7, 134.3, 134.5, 134.8, 135.5, 135.7, 136.4, 136.5, 137.9, 138.1, 139.8, 140.2, 150.9, 155.6, 156.8, 158.8, 159.3 ppm. MALDI-TOF: m/z (%) = 686.8 (100) $[M - 28]^+$. $C_{47}H_{33}N_5OS$ (715.86): calcd. C 78.86, H 4.65, N 9.78, S 4.48; found C 78.90, H 4.60, N 9.83, S 4.40.

General Synthesis of Click Porphyrin Dyads 1–6 and Porphyrin–Ferrocene Click Conjugates 7–11: Samples of one equivalent of *meso*-(azidophenyl)porphyrin and one equivalent of ethynylferrocene or ethynylporphyrin were dissolved in 1:1 mixture of THF/CH_3CN under nitrogen atmosphere with stirring at room temperature. To this 1 equiv. of diisopropylethylamine (DIPEA) was added followed by the addition of CuI (0.1 equiv.) and continued stirring for 12 h. Progress of the reaction was monitored by periodic tlc analysis. The solvent was removed under reduced pressure and the crude mixture was subjected to basic alumina flash column chromatography. The small amounts of unreacted precursors were removed with dichloromethane and the desired fraction of the click porphyrin dyad/ferrocene conjugate was eluted with 1–2% methanol in dichloromethane and the resulting compound was recrystallised from dichloromethane/hexane to give the desired products as brownish red solid in 46–52% yields.

ZnN_4–N_3S Porphyrin Click Dyad (1): Yield 50%; m.p. >300 °C. ^{1}H NMR (400 MHz, $CDCl_3$): δ = –2.65 (s, 1 H, NH), 2.72 (s, 18 H, CH_3), 7.52–7.58 (m, 12 H, Ar), 7.65 (d, J = 7.9 Hz, 2 H, Ar), 8.08–8.18 (m, 14 H, Ar), 8.38–8.44 (m, 4 H, Ar + β-pyrrole), 8.51 (d, J = 8.5 Hz, 2 H, Ar), 8.64 (d, J = 4.5 Hz, 1 H, β-pyrrole), 8.71–8.72 (m, 2 H, β-pyrrole), 8.74 (d, J = 4.5 Hz, 1 H, β-pyrrole), 8.79 (s, 1 H, triazole), 8.97–9.03 (m, 4 H, β-pyrrole), 9.02 (d, J = 4.5 Hz, 2 H, β-pyrrole), 9.06 (d, J = 4.5 Hz, 2 H, β-pyrrole), 9.79 (d, J = 5.1 Hz, 1 H, β-thiophene), 9.84 (d, J = 5.1 Hz, 1 H, β-thiophene) ppm. MALDI-TOF: m/z (%) = 1428.6 (100) $[M - 28]^+$. $C_{96}H_{68}N_{10}SZn$ (1456.46): calcd. C 79.02, H 4.70, N 9.60, S 2.20; found C 79.05, H 4.68, N 9.62, S 2.17.

ZnN_4–N_2S_2 Porphyrin Click Dyad (2): Yield 48%; m.p. >300 °C. ^{1}H NMR (400 MHz, $CDCl_3$): δ = 2.72 (s, 18 H, CH_3), 7.57 (d, J = 7.3 Hz, 6 H, Ar), 7.65 (d, J = 7.3 Hz, 6 H, Ar), 8.10–8.16 (m, 12 H, Ar), 8.39–8.42 (m, 6 H, Ar), 8.49 (d, J = 8.2 Hz, 2 H, Ar), 8.71 (s, 2 H, β-pyrrole), 8.73 (d, J = 3.9 Hz, 1 H, β-pyrrole), 8.76 (d, J = 3.9 Hz, 1 H, β-pyrrole), 8.79 (s, 1 H, triazole), 8.96 (s, 4 H, β-pyrrole), 9.01 (d, J = 4.5 Hz, 2 H, β-pyrrole), 9.03 (d, J = 4.5 Hz, 2 H, β-pyrrole), 9.73–9.77 (m, 4 H, β-thiophene) ppm. MALDI-TOF: m/z (%) = 1446.8 (100) $[M - 28]^+$. $C_{96}H_{67}N_9S_2Zn$ (1473.43): calcd. C 78.11, H 4.57, N 8.54, S 4.35; found C 78.14, H 4.54, N 8.52, S 4.37.

ZnN_4–N_2SO Porphyrin Click Dyad 3: Yield 46%; m.p. >300 °C. ^{1}H NMR (400 MHz, $CDCl_3$): δ = 2.72 (s, 18 H, CH_3), 7.57 (m, 10 H, Ar), 7.63 (d, J = 8.2 Hz, 2 H, Ar), 8.01 (d, J = 8.2 Hz, 1 H, Ar), 8.05–8.15 (m, 12 H, Ar), 8.25 (d, J = 7.6 Hz, 1 H, Ar), 8.37 (d, J = 8.2 Hz, 2 H, Ar), 8.41 (d, J = 8.8 Hz, 2 H, Ar), 8.43 (d, J = 4.5 Hz, 1 H, β-pyrrole), 8.48 (d, J = 8.5 Hz, 2 H, Ar), 8.49 (d, J = 4.5 Hz, 1 H, β-pyrrole), 8.57 (d, J = 4.5 Hz, 1 H, β-pyrrole), 8.61 (d, J = 4.5 Hz, 1 H, β-pyrrole), 8.78 (s, 1 H, triazole), 8.94–9.08 (m, 8 H, β-pyrrole), 9.21 (s, 2 H, β-furan), 9.74 (d, J = 5.1 Hz, 1 H, β-thiophene), 9.79 (d, J = 5.1 Hz, 1 H, β-thiophene) ppm. MALDI-TOF: m/z (%) = 1429.25 (100) $[M - 28]^+$. $C_{96}H_{67}N_9OSZn$ (1457.45): calcd. C 78.97, H 4.63, N 8.63, S 2.21; found C 78.95, H 4.65, N 8.65, S 2.19.

Demetallated dyads **4** and **5** can be obtained by treating dichloromethane solution of zinc dyads **1** and **2** (10 mg in 10 mL of dichloromethane) with minute amount of trifluoroacetic acid (0.1 mL) at room temperature followed by neutralization with triethylamine. The resulting compound was passed through a small plug of basic alumina to get pure demetallated dyads in quantitative yields.

N_4-N_3S Porphyrin Click Dyad 4: M.p. >300 °C. ^{1}H NMR (400 MHz, $CDCl_3$): δ = –2.73 (s, 2 H, NH), –2.65 (s, 1 H, NH), 2.72 (s, 18 H, CH_3), 7.57 (d, J = 7.6 Hz, 10 H, Ar), 7.65 (d, J = 7.9 Hz, 2 H, Ar), 8.08–8.13 (m, 12 H, Ar), 8.16 (d, J = 7.9 Hz, 2 H, Ar), 8.32–8.42 (m, 6 H, Ar), 8.48 (m, 2 H, β-pyrrole), 8.64 (d, J = 4.5 Hz, 1 H, β-pyrrole), 8.69–8.79 (m, 4 H, triazole + β-pyrrole), 8.86–8.98 (m, 8 H, β-pyrrole), 9.79 (d, J = 5.1 Hz, 1 H, β-thiophene), 9.84 (d, J = 5.1 Hz, 1 H, β-thiophene) ppm. MALDI-TOF: m/z (%) = 1366.65 (100) $[M - 28]^+$. $C_{96}H_{70}N_{10}S$ (1394.55): calcd. C 82.61, H 5.06, N 10.03, S 2.30; found C 82.60, H 5.08, N 10.04, S 2.28.

N_4-N_2S_2 Porphyrin Click Dyad 5: M.p. >300 °C. ^{1}H NMR (400 MHz, $CDCl_3$): δ = –2.73 (s, 2 H, NH), 2.72 (s, 18 H, CH_3), 7.57 (d, J = 7.3 Hz, 6 H, Ar), 7.65 (d, J = 7.3 Hz, 6 H, Ar), 8.10–8.17 (m, 12 H, Ar), 8.36–8.44 (m, 6 H, Ar), 8.49 (d, J = 8.2 Hz, 2 H, Ar), 8.70–8.79 (m, 5 H, triazole + β-pyrrole), 8.88 (s, 4 H, β-pyrrole), 8.92 (d, J = 4.5 Hz, 2 H, β-pyrrole), 8.96 (d, J = 4.5 Hz, 2 H, β-pyrrole), 9.71–9.74 (m, 3 H, β-thiophene), 9.79 (d, J = 5.1 Hz, 1 H, β-thiophene) ppm. MALDI-TOF: m/z (%) = 1383.61 (100) $[M - 28]^+$. $C_{96}H_{69}N_9S_2$ (1411.51): calcd. C 81.62, H 4.92, N 8.92, S 4.54; found C 81.64, H 4.91, N 8.93, S 4.52.

N_3S-N_2S_2 Porphyrin Click Dyad 6: Yield 46%; m.p. >300 °C. ^{1}H NMR (400 MHz, $CDCl_3$): δ = –2.64 (s, 1 H, NH), 2.72 (s, 18 H, CH_3), 7.52–7.58 (m, 4 H, Ar), 7.64 (d, J = 7.9 Hz, 10 H, Ar), 8.06–8.18 (m, 12 H, Ar), 8.38–8.52 (m, 6 H, Ar), 8.63 (d, J = 4.5 Hz, 1 H, β-pyrrole), 8.68 (d, J = 4.2 Hz, 1 H, β-pyrrole), 8.71–8.73 (m, 4 H, β-pyrrole), 8.74 (d, J = 4.5 Hz, 1 H, β-pyrrole), 8.78 (s, 1 H,

triazole), 8.80 (d, J = 4.5 Hz, 1 H, β-pyrrole), 8.94–8.98 (m, 2 H, β-pyrrole), 9.72–9.86 (m, 6 H, β-thiophene) ppm. MALDI-TOF: m/z (%) = 1399.87 (100) $[M - 28]^+$. $C_{96}H_{68}N_8S_3$ (1428.47): calcd. C 80.64, H 4.79, N 7.84, S 6.73; found C 80.66, H 4.77, N 7.85, S 6.72.

ZnN_4-Ferrocene Click Conjugate 7: Yield 50%; m.p. >300 °C. ^{1}H NMR (400 MHz, $CDCl_3$): δ = 2.72 (s, 9 H, CH_3), 4.27 (s, 5 H, ferrocene), 4.45 (t, J = 1.8 Hz, 2 H, ferrocene), 5.22 (t, J = 1.8 Hz, 2 H, ferrocene), 7.56 (d, J = 6.7 Hz, 6 H, Ar), 7.97 (d, J = 8.5 Hz, 1 H, Ar), 8.09–8.12 (m, 6 H, Ar), 8.19 (d, J = 8.5 Hz, 1 H, Ar), 8.21 (s, 1 H, triazole), 8.40 (d, J = 8.5 Hz, 1 H, Ar), 8.42 (d, J = 8.5 Hz, 1 H, Ar), 8.94–9.05 (m, 8 H, β-pyrrole) ppm. ^{13}C NMR (100 MHz, $CDCl_3$): δ = 21.9, 52.3, 52.9, 53.6, 67.1, 68.0, 69.6, 70.0, 110.1, 118.7, 121.6, 121.8, 123.9, 124.2, 124.9, 127.2, 127.7, 128.3, 131.3, 132.2, 132.7, 134.2, 134.8, 135.0, 136.4, 137.3, 139.9, 145.2, 149.8, 150.5, 150.7 ppm. ES MS: m/z (%) = 971.53 (100) $[M]^+$. $C_{59}H_{43}FeN_7Zn$ (971.27): calcd. C 72.96, H 4.46, N 10.09; found C 72.98, H 4.47, N 10.06.

N_4-Ferrocene Click Conjugate 8: M.p. >300 °C. ^{1}H NMR (400 MHz, $CDCl_3$): δ = –2.76 (s, 1 H, NH), 2.71 (s, 9 H, CH_3), 4.27 (s, 5 H, ferrocene), 4.45 (t, J = 1.8 Hz, 2 H, ferrocene), 5.21 (t, J = 1.8 Hz, 2 H, ferrocene), 7.56 (d, J = 6.4 Hz, 6 H, Ar), 7.97 (d, J = 8.2 Hz, 2 H, Ar), 8.09–8.11 (m, 6 H, Ar), 8.20 (s, 1 H, triazole), 8.42 (d, J = 8.2 Hz, 2 H, Ar), 8.87–8.94 (m, 8 H, β-pyrrole) ppm. ^{13}C NMR (100 MHz, $CDCl_3$): δ = 21.7, 67.0, 67.6, 69.2, 69.8, 100.3, 120.6, 124.4, 124.8, 127.6, 134.7, 135.3, 137.6, 139.2, 144.5, 158.2 ppm. ES MS: m/z (%) = 908.14 (100) $[M]^+$. $C_{59}H_{45}FeN_7$ (907.88): calcd. C 78.05, H 5.00, N 10.80; found C 78.03, H 5.02, N 10.80.

N_3S-Ferrocene Click Conjugate 9: Yield 52%; m.p. >300 °C. ^{1}H NMR (400 MHz, $CDCl_3$): δ = –2.68 (s, 1 H, NH), 2.71 (s, 9 H, CH_3), 4.20 (s, 5 H, ferrocene), 4.41 (s, 2 H, ferrocene), 4.91 (s, 2 H, ferrocene), 7.56 (d, J = 7.9 Hz, 4 H, Ar), 7.63 (d, J = 7.6 Hz, 2 H, Ar), 8.08 (d, J = 7.9 Hz, 4 H, Ar), 8.14 (d, J = 7.9 Hz, 2 H, Ar), 8.20 (s, 1 H, triazole), 8.25 (d, J = 8.5 Hz, 2 H, Ar), 8.43 (d, J = 8.5 Hz, 2 H, Ar), 8.62 (d, J = 4.5 Hz, 1 H, β-pyrrole), 8.66–8.72 (m, 3 H, β-pyrrole), 8.96 (m, 2 H, β-pyrrole), 9.72 (d, J = 5.1 Hz, 1 H, β-thiophene), 9.80 (d, J = 5.1 Hz, 1 H, β-thiophene) ppm. ^{13}C NMR (100 MHz, $CDCl_3$): δ = 21.7, 67.0, 69.1, 69.8, 116.9, 119.5, 121.4, 124.3, 126.0, 127.5, 128.5, 129.1, 129.2, 132.0, 132.6, 133.3, 133.6, 134.3, 134.5, 134.8, 135.4, 135.8, 136.0, 136.9, 137.8, 138.1, 139.3, 139.5, 141.7, 144.8, 145.7, 147.1, 148.0, 148.2, 153.7, 154.7, 157.0, 157.8 ppm. ES MS: m/z (%) = 925.14 (100) $[M]^+$. $C_{59}H_{44}FeN_6S$ (924.93): calcd. C 76.61, H 4.79, N 9.09, S 3.47; found C 76.62, H 4.80, N 9.08, S 3.46.

N_2S_2-Ferrocene Click Conjugate 10: Yield 51%; m.p. >300 °C. ^{1}H NMR (400 MHz, $CDCl_3$): δ = 2.71 (s, 9 H, CH_3), 4.27 (s, 5 H, ferrocene), 4.45 (t, J = 1.8 Hz, 2 H, ferrocene), 5.22 (t, J = 1.8 Hz, 2 H, ferrocene), 7.63 (d, J = 7.6 Hz, 6 H, Ar), 8.03 (d, J = 8.2 Hz, 1 H Ar), 8.13 (d, J = 7.6 Hz, 6 H, Ar), 8.19 (s, 1 H, triazole), 8.24 (d, J = 8.2 Hz, 1 H, Ar), 8.40–8.45 (m, 2 H, Ar), 8.67–8.78 (m, 4 H, β-pyrrole), 9.65–9.78 (m, 4 H, β-thiophene) ppm. ^{13}C NMR (100 MHz, $CDCl_3$): δ = 21.7, 67.6, 69.8, 69.9, 119.4, 125.5, 128.4, 134.4, 134.7, 134.9, 135.4, 135.9, 136.8, 138.0, 138.4, 147.8, 148.1, 148.3, 156.7 ppm. ES MS: m/z (%) = 941.81 (100) $[M]^+$. $C_{59}H_{43}FeN_5S_2$ (941.98): calcd. C 75.23, H 4.60, N 7.43, S 6.81; found C 75.24, H 4.61, N 7.41, S 6.81.

N_2SO-Ferrocene Click Conjugate 11: Yield 48%; m.p. >300 °C. ^{1}H NMR (400 MHz, $CDCl_3$): δ = 2.70 (s, 9 H, CH_3), 4.20 (s, 5 H, ferrocene), 4.41 (t, J = 1.8 Hz, 2 H, ferrocene), 4.90 (t, J = 1.8 Hz, 2 H, ferrocene), 7.55 (d, J = 7.6 Hz, 4 H, Ar), 7.62 (d, J = 7.6 Hz, 2 H, Ar), 8.05 (d, J = 7.6 Hz, 4 H, Ar), 8.10–8.13 (m, 2 H, Ar), 8.19 (s, 1 H, triazole), 8.24 (d, J = 8.5 Hz, 2 H, Ar), 8.39–8.49 (m, 4 H, 2β-pyrrole + 2Ar), 8.54–8.60 (m, 2 H, β-pyrrole), 9.19 (s, 2 H, β-furan), 9.68 (d, J = 4.8 Hz, 1 H, β-thiophene), 9.75 (d, J = 5.1 Hz, 1 H, β-thiophene) ppm. ^{13}C NMR (100 MHz, $CDCl_3$): δ = 21.7, 67.1, 67.6, 69.1, 69.9, 116.9, 119.5, 121.4, 125.6, 127.8, 128.5, 129.9, 131.6, 133.1, 133.7, 134.5, 135.0, 135.5, 135.7, 136.8, 137.8, 138.1, 139.7, 141.4, 148.2, 150.9, 155.6, 156.8, 159.4 ppm. ES MS: m/z (%) = 925.72 (100) $[M]^+$. $C_{59}H_{43}FeN_5OS$ (925.92): calcd. C 76.53, H 4.68, N 7.56, S 3.46; found C 76.55, H 4.67, N 7.55, S 3.46.

Supporting Information (see also the footnote on the first page of this article): NMR and mass spectra of selected compounds.

Acknowledgments

M. R. thanks the Council of Scientific and Industrial Research (CSIR) and Department of Science and Technology (DST) for financial support and V. S. thanks the CSIR for a fellowship.

[1] H. C. Kolb, M. G. Finn, K. B. Sharpless, *Angew. Chem. Int. Ed.* **2001**, *40*, 2004–2021.
[2] a) V. D. Bock, H. Hiemstra, J. H. van Maarseveen, *Eur. J. Org. Chem.* **2006**, 51–68; b) J. E. Moses, A. D. Moorhouse, *Chem. Soc. Rev.* **2007**, *36*, 1249–1262; c) M. Meldal, C. W. Tornoe, *Chem. Rev.* **2008**, *108*, 2952–3015.
[3] a) C. Maeda, S. Yamaguchi, C. Ikeda, H. Shinokubo, A. Osuka, *Org. Lett.* **2008**, *10*, 549–552; b) F. C. Santos, A. C. Cunha, M. B. V. de Souza, A. C. Tome, M. G. P. M. S. Neves, V. F. Ferreira, J. A. S. Cavaleiro, *Tetrahedron Lett.* **2008**, *49*, 7268–7270; c) Y. Ikawa, H. Harada, M. Toganoh, H. Furuta, *Bioorg. Med. Chem. Lett.* **2009**, *19*, 2448–2452.
[4] a) D.-M. Shen, C. Liu, Q.-Y. Chen, *Eur. J. Org. Chem.* **2007**, 1419–1422; b) M. Severac, L. L. Pleux, A. Scarpaci, E. Blart, F. Odobel, *Tetrahedron Lett.* **2007**, *48*, 6518–6522; c) S. Punidha, J. Sinha, A. Kumar, M. Ravikanth, *J. Org. Chem.* **2008**, *73*, 323–326.
[5] a) I. Gupta, M. Ravikanth, *J. Org. Chem.* **2004**, *69*, 6796–6811; b) S. Punidha, N. Agarwal, M. Ravikanth, *Eur. J. Org. Chem.* **2005**, 2500–2517; c) S. Punidha, N. Agarwal, I. Gupta, M. Ravikanth, *Eur. J. Org. Chem.* **2007**, 1168–1175; d) S. Rai, M. Ravikanth, *Tetrahedron* **2007**, *63*, 2455–2465.
[6] B. Karine, A. D. Moorhouse, J. E. Moses, *Org. Lett.* **2007**, *9*, 1809–1811.
[7] X. Liu, J. Liu, K. Jin, X. Yang, Q. Peng, L. Sun, *Tetrahedron* **2005**, *61*, 5655–5662.
[8] S. Shanmugathasan, C. Edwards, R. W. Boyle, *Tetrahedron* **2000**, *56*, 1025–1046.
[9] J. S. Lindsey, I. C. Schreiman, H. C. Hsu, P. C. Kearney, A. M. Marguerettaz, *J. Org. Chem.* **1987**, *52*, 827–836.
[10] S. Punidha, M. Ravikanth, *Synlett* **2005**, *14*, 2199–2203.
[11] P. Y. Heo, C. H. Lee, *Bull. Korean Chem. Soc.* **1996**, *17*, 515–520.
[12] L. Latos-Grazynski, *Core-Modified Heteroanalogues of Porphyrins and Metalloporphyrins*, in: *The Porphyrin Handbook* (Eds.: K. M. Kadish, K. M Smith, R. Guilard), Academic Press, New York, **2000**; vol. 2, p. 361–416.
[13] R. S. Loewe, R. K. Lammi, J. R. Diers, C. Kirmaier, D. F. Bocian, D. Holten, J. S. Lindsey, *J. Mater. Chem.* **2002**, *12*, 1530–1552.
[14] N. F. Langille, T. F. Jamison, *Org. Lett.* **2006**, *8*, 3761–3764.
[15] I. Gupta, M. Ravikanth, *Coord. Chem. Rev.* **2006**, *250*, 468–518.
[16] C.-H. Hung, C.-K. Ou, G.-H. Lee, S.-M. Peng, *Inorg. Chem.* **2001**, *40*, 6845–6847.
[17] a) P. D. W. Boyd, A. K. Burrell, W. M. Campbell, P. A. Cocks, K. C. Gordon, G. B. Jameson, D. L. Officer, Z. Zhao, *Chem. Commun.* **1999**, 637–638; b) D. T. Gryko, F. Zhao, A. A. Yas-

seri, K. M. Roth, D. F. Bocian, W. G. Kuhr, J. S. Lindsey, *J. Org. Chem.* **2000**, *65*, 7356–7362; c) S. Rai, G. Gayatri, G. N. Sastry, M. Ravikanth, *Chem. Phys. Lett.* **2008**, *467*, 179–185.
[18] B. Koszarna, H. Butenschön, D. T. Gryko, *Org. Biomol. Chem.* **2005**, *3*, 2640–2645.
[19] K. M. Kadish, E. Caemelbecke, *J. Solid State Electrochem.* **2003**, *7*, 254–258.
[20] I. Gupta, M. Ravikanth, *Inorg. Chim. Acta* **2007**, *360*, 1731–1742.
[21] D. Kumaresan, A. Datta, M. Ravikanth, *Chem. Phys. Lett.* **2004**, *395*, 87–91.

Received: September 21, 2009
Published Online: December 10, 2009

